INCO-CT-2004-509093

ADU-RES

Co-ordination Action for Autonomous Desalination Units based on Renewable Energy Systems

Work Package 6

Further Development of Integrated Plant Design

Deliverable 6.1

Energy Consumption Modelling

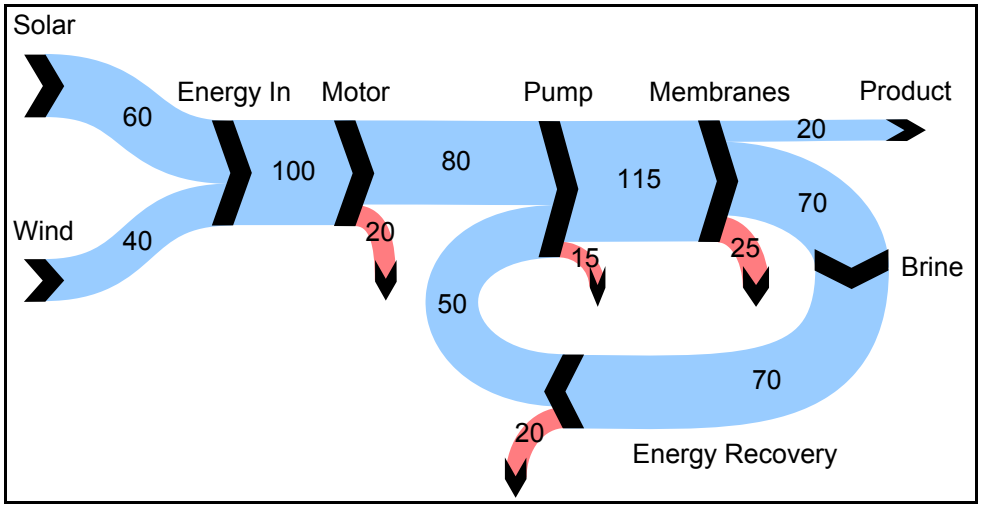

CREST UK, October 2006

Work Package 6 Participants

Organization	Participant Researchers
CREST, Loughborough University, U.K.	Murray Thomson Alfredo Bermudez David Infield
Fraunhofer ISE, Germany	Joachim Went
Agricultural University of Athens (AUA), Greece	Costas Soulis
Centre for Renewable Energy Sources, (CRES), Greece	Eftihia Tzen
Joint Research Centre (JRC), EU	Neringa Narbutiene Robert Edwards
Instituto Tecnológico de Canarias, (ITC), Spain	Baltasar Peñate Suarez Vicente Subiela Ortin Gonzalo Piernavieja Izquierdo

Project Coordination
Dr Christian Epp
Michael Papapetrou
WIP – Renewable Energies
Sylvensteinstrasse 2, 81369 Munich, Germany
christian.epp@wip-munich.de
michael.papapetrou@wip-munich.de
Tel: 0049 89 720 12 735

This report prepared by
Murray Thomson
Alfredo Bermudez
CREST (Centre for Renewable Energy Systems Technology)
Loughborough University
Loughborough, LE11 3TU, United Kingdom
M.Thomson@Lboro.ac.uk
Tel: 0044 1509 228144

with specific technical assistance from
Eftihia Tzen
Centre for Renewable Energy Sources, (CRES)
Greece

and
Vicente Subiela Ortin
Baltasar Peñate Suarez
Instituto Tecnológico de Canarias (ITC)
Pozo Izquierdo, Gran Canaria Island

Contents

1 Introduction

Many demonstration ADU-RES systems have been constructed and operated in recent years. In all cases, the quantity of water produced is modest in relation to the size of the solar collectors, wind-turbines or other renewable-energy collection equipment. Ultimately, this makes the water expensive and is the main factor constraining the commercial uptake of ADU-RES.

The problem is largely due to energy losses in each of the individual components that make up ADU-RES systems. In fairness, similar losses are also prevalent in small-scale fossil-fuelled desalination systems, but often go unnoticed because the capital costs of internal combustion engines (or alternatives) are relatively low.

This report presents modelling of energy flows in a selection of ADU-RES systems. The aim is to quantify the energy losses in the various components and thus indicate where attention should be focused in order to reduce those losses in future system designs.

The selected systems include solar photovoltaics (PV) and wind power; they are all based on reverse osmosis (RO).

2 Energy in RO systems

This section describes the fundamentals of energy consumption in RO systems.

2.1 Concentration

The concentration of salts in the feed water is the primary factor determining the energy required for desalination.

Average seawater has a total-dissolved-solids concentration of 35 750 mg/L. Some seas have significantly higher concentrations, notably the Red Sea and Arabian Gulf, which can be up to 45 000 mg/L, and therefore require more energy to desalinate.

Brackish groundwaters (concentrations typically less than 10 000 mg/L) generally require much less energy.

2.2 Osmotic pressure

Osmotic pressure is roughly proportional to concentration.

The exact relationship is a complex function of the concentrations of each of the ions present in the water, but for a basic appreciation of energy flows, it is sufficient to know that doubling the concentration will roughly double the osmotic pressure, and a similar doubling of energy consumption can be expected.

2.3 Theoretical minimum desalination energy

The theoretical minimum energy required to remove salt from water is independent of the method employed and is directly related to the osmotic pressure:

$$1 \text{ bar} = 1/36 \text{ kWh/m}^3$$

Average seawater has an osmotic pressure of around 26 bar, which equates to just over 0.7 kWh/m^3.

In practice however, the osmotic pressure increases as the desalination takes place: the removal of fresh water causes the feed water to become concentrated. Thus, the energy required to remove the salt increases, depending on the recovery ratio, as indicated in Figure 1.

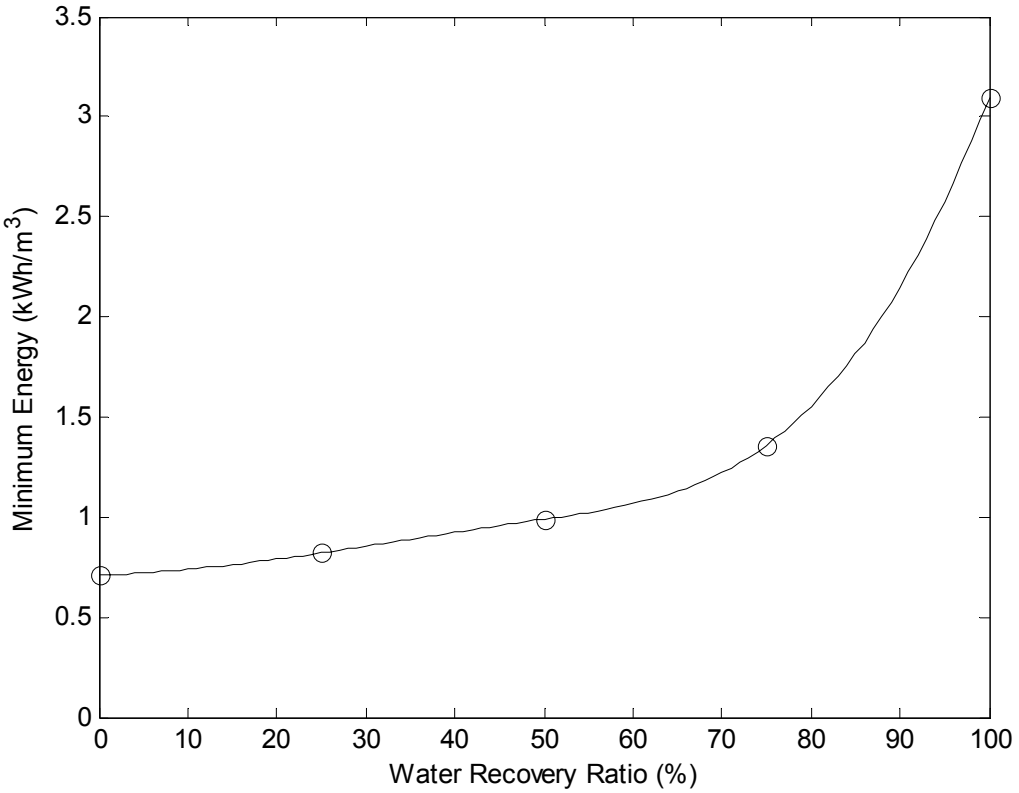

Figure 1 – Theoretical minimum energy required to desalinate seawater at 25 ºC [1]

The above discussion, including Figure 1, refers to the complete removal of salt, which is not generally necessary in the production of drinking water. Product concentrations of up to 600 mg/L can be acceptable and this slightly reduces the energy required. The reduction is usually insignificant in seawater systems but is worth noting in the case of brackish water.

The temperature of the water also has a slight affect: osmotic pressure is roughly proportional to absolute temperature in Kelvin. This factor is generally insignificant in RO systems and should not be confused with the temperature dependence of RO membranes.

2.4 Pre-treatment losses

Almost all practical RO systems include some form of pre-treatment. Usually, this includes filtration, and requires energy to overcome the associated pressure drops. Provided that filters are appropriately sized and properly maintained, the energy required is generally small compared to that for the actual desalination and is not included in the modelling presented here.

[1] Johnson, James S., Lawrence Dresner and Kurt A. Kraus (1966). Hyperfiltration (Reverse Osmosis). *Principles of Desalination*. K. S. Spiegler. New York, Academic Press, page 357.

2.5 Membrane losses

Energy losses in RO membranes can be divided into through-flow losses and cross-flow losses.

Through-flow losses

An ideal RO membrane would form a complete barrier to salt ions but would allow water to pass through freely. In this case, the energy consumption would be solely due to the osmotic pressure, as discussed above. With a real membrane however, the feed pressure has to be greater than the osmotic pressure in order to push the water through the membrane. This additional pressure is known as the “net driving pressure” and corresponds to additional energy, which is dissipated as heat and lost.

This energy loss is proportional to the net driving pressure and can thus be reduced by reducing the system feed pressure. To minimise the energy loss, the system feed pressure should be only slightly above the osmotic pressure of the concentrate, and it is notable that the (traditionally powered) RO systems with the lowest energy consumptions do operate at relatively low pressures.

On the other hand, the flow (quantity) of product water is also roughly proportional to the net driving pressure, and thus, the system designer must balance the conflicting objectives of minimising the energy losses described above against maximising the product flow.

The situation can be improved by use of a large membrane area (extra membrane modules), and again, it is notable that RO systems designed to minimise energy consumption do tend to have a generous number of modules. The benefit of reduced energy costs has to be set against the increased capital and replacement costs of membranes, and an increase in product concentration.

Membrane manufactures also seek to minimise the energy loss described above, by designing membranes to allow water to pass through as freely as possible. Membranes designed with this priority are described as “high-flow” or “low-pressure” membranes. Unfortunately, but unsurprisingly, these membranes also tend to allow slightly more salt to pass through. Membranes designed to minimise salt passage are described as “high-rejection”, and are less energy efficient.

Cross-flow losses

Cross-flow losses correspond to the pressure drop between the feed inlet to the membranes and the concentrate outlet, sometimes known as the “delta pressure”.

In energy terms, cross-flow losses are usually small in comparison to through-flow losses.

Through-flow and cross-flow losses are calculated separately in the modelling described in this report, but they are combined in the presented results.

2.6 Concentrate energy

The concentrate exiting the membranes of an RO system has hydraulic energy by virtue of its flow and pressure.

In seawater systems, this energy is very significant: typically equal to around two thirds of the energy presented to the membranes at the feed intake.

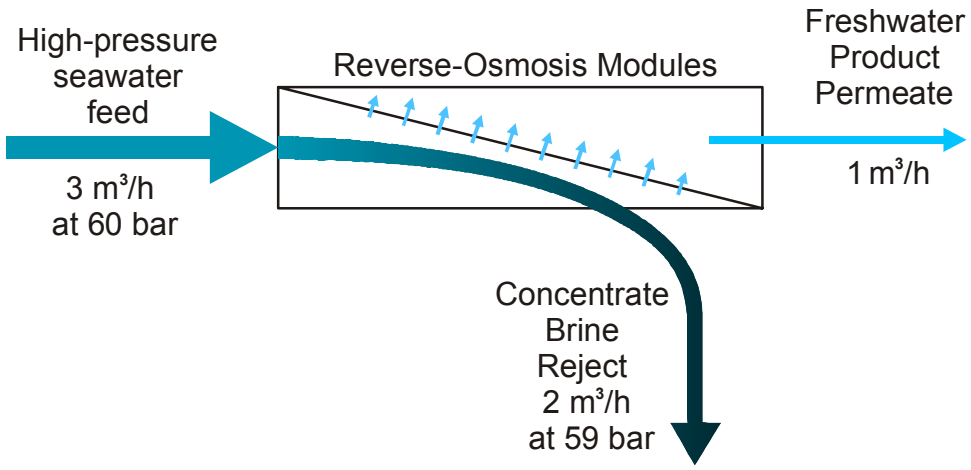

Figure 2 – Example to illustrate concentrate energy in seawater RO

Large and medium-scale (traditionally powered) seawater RO systems are almost always equipped with “brine-stream energy recovery”. The traditional mechanism was a Pelton wheel coupled to the shaft of the main feed pump.

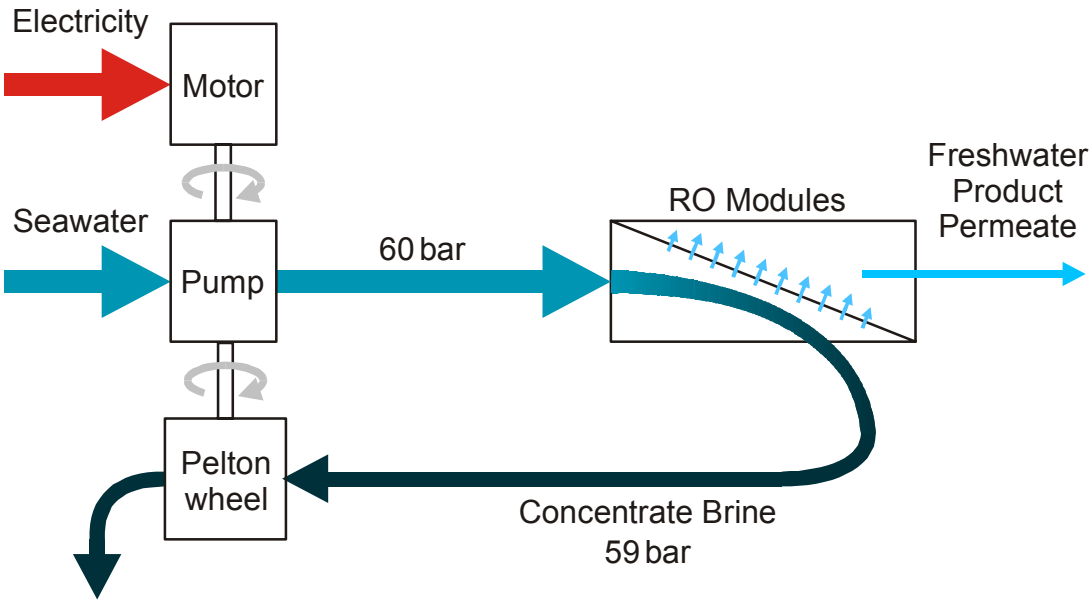

Figure 3 – Use of a Pelton wheel in a large (traditionally powered) RO system

In recent years, alternative brine-stream energy recovery mechanisms have been developed and widely employed in large and medium-scale RO systems. These include the DWEER Work Exchanger[2] and the ERI Pressure Exchanger[3].

Unfortunately, the devices mentioned above are not readily available at small-scale (product flow below ~ 50 m^3/d) and the vast majority of small-scale RO systems are fitted with a needle valve to provide the necessary backpressure to the membranes. The concentrate energy is dissipated as heat in the needle valve and lost. As a result, the relative energy consumption in these systems is very high.

Various devices have been developed for and applied to brine-stream energy recovery in small-scale RO systems. These include the Clark pump[4], which has been very successful in use on leisure yachts, and the Danfoss axial-piston motor (APM)[5]. Unfortunately, these devices cost rather more than a simple needle valve and their potential to save on-going energy costs is often overlooked.

Brackish water RO systems usually operate at a higher (water) recovery ratio than seawater systems. Thus, the proportion of the energy in the concentrate is lower and the importance of brine-stream energy recovery is reduced.

[2] www.calder.ch
[3] www.energy-recovery.com
[4] www.spectrawatermakers.com
[5] http://nessie.danfoss.com

2.7 Specific energy (kWh/m^3)

Dividing the energy consumption of an RO plant in kW by the product flow in m^3/h yields the "specific energy" in kWh/m^3, and provides a convenient basis for comparing energy consumption in plants of different capacities. Some typical figures are given in Table 1.

	Specific energy (kWh/m^3)
Without energy recovery	5 – 10
With energy recovery	2 – 4
Theoretical minimum	~ 1

Table 1 – Typical energy consumptions for medium and large-scale traditionally powered seawater RO

It should be emphasised however that specific energy figures depend greatly on where the energy is being measured and what it includes. In a grid-powered RO system, the designer may focus on the energy consumption of the motor driving main high-pressure-pump and perhaps overlook auxiliary loads such as a well pump. With an autonomous system on the other hand, there is a greater obligation to include all aspects of energy consumption, and thus, specific energy figures will appear higher.

System size also has a significant bearing on specific energy consumption. The energy efficiencies of small electric motors and pumps are very much less than larger machines. Also, parasitic losses, such as measurement and control equipment, will be a more significant proportion of the total energy consumption. Fortunately, the energy efficiency of the membranes themselves is almost unaffected by system size: the membrane material used in a single 2.5-inch or 4-inch element in a very small RO system is identical to that used in the multiple 8-inch to 18-inch elements of a municipal RO system. The care and cleaning of the membranes however, which is required equally in all systems, might not be carried out so carefully carried out in small systems, and this will lead to a more rapid decline in performance, including a rise in specific energy.

3 Modelling methodology

The software models presented in this report are intended to simulate the energy flows and water production of the real demonstration systems on which they are based. The models are based on information taken from numerous published and unpublished sources. In many cases, additional information was required in order to complete the model and assumptions were made. The assumed details are described for each of the modelled systems. This section describes the general approach to the modelling of all systems.

3.1 Software

The models are written in Matlab-Simulink, which is a general-purpose simulation tool used worldwide in engineering and academic research. It can be used to develop very detailed time-step simulations of complex physical systems, and is vastly more powerful than Excel. Of course the quality of the results is still critically dependent on the quality of the model construction and the data used as input.

The general arrangement of the Matlab-Simulink models follows the approach taken previously by Thomson[6] and Miranda[7], which proved very successful in predicting specific energy consumption of the ADU-RES system at CREST.

This approach to the modelling allows the behaviour of each component to be represented in detail. For example, the model of a centrifugal pump can include accurate pressure-flow and energy-efficiency curves representing the full range of its operation. A simple model constructed in Excel would tend to use single-point parameters, which may not be accurate when the pump is operated under differing conditions.

Matlab-Simulink facilitates time-series simulation, and the models presented in this report are configured to simulate hour-by-hour operation for a complete year. This level of detail is important in order to accurately represent the operation of ADU-RES systems with variable energy inputs. In systems with batteries, the state-of-charge and cell voltages are calculated at each time step and used to determine the on/off operation of the RO section. In systems without batteries, flows and pressures throughout the RO section vary in

[6] Thomson, Murray (2004). *Reverse-Osmosis Desalination of Seawater Powered by Photovoltaics Without Batteries*, PhD, University of Loughborough, UK. http://www-staff.lboro.ac.uk/~elmt/Thesis.htm

[7] Miranda, Marcos S. (2003). *Small-Scale Wind-Powered Seawater Desalination Without Batteries*, PhD, Loughborough University, UK. http://staff.bath.ac.uk/eesmm/Thesis.html

response to the variable energy input and this is fully represented in the modelling.

Selection of a 1-hour time-step facilitates simulation of a whole year of operation so that seasonal and weather variations can be represented. Variations occurring within an hour, such as passing clouds affecting the solar input and wind turbulence, are not represented, but trial simulation runs using shorter time-steps have shown no significant differences in overall results.

3.2 Input data

The real demonstration systems (on which the models are based) are located in various countries, and naturally, their performance is very dependent on local conditions:

- Solar radiation
- Wind speed
- Feed water concentration and temperature
- Ambient temperature

The software models use hourly data to represent these variables, and the details of the data sources are given in the "assumed data" section for each system.

3.3 Photovoltaics (PV)

Ambient temperature and solar radiation data is used to model cell temperature using NOCT[8]. The operation of each PV cell is then represented by a one or two-diode model, calibrated to match the manufacturer's published current-voltage (I-V) curves for the module.

The series-parallel configuration of the array is represented by simple multiplication of currents and voltages. No allowance is made for mismatch and shading losses; these losses should be small provided that good-quality modules are installed in open aspect and kept clean.

3.4 Maximum power point tracking (MPPT)

The maximum power point is determined from the I-V curve mentioned above. The model assumes that the tracking algorithm is perfect: no tracking errors. Losses in the DC-DC or DC-AC power-electronic converter are modelled appropriately.

[8] *Normal Operating Cell Temperature* (NOCT), see Markvart, Tomas (1999), *Solar Electricity*. Chichester, Wiley, page 88.

3.5 Charge controllers

Charge controllers do not perform maximum power point tracking; they simply disconnect the PV from the battery when the state-of-charge (indicated by the battery voltage) exceeds a threshold and thus prevent overcharging. Some charge controllers use pulse-width modulation (PWM) to provide float and equalisation charging, but as the model operates on a 1-hour time-step, these details of are not of importance here.

In a PV-RO system, a charge controller serves only as a backup to prevent overcharging: in normal operation, the RO rig will be switched on at a threshold below that of the charge controller. Thus, it was not necessary to specifically include charge controllers in the models.

In the absence of maximum power point tracking, the battery voltage is simply applied to the PV, and the current at that voltage is calculated from the I-V curve mentioned above. In general, the battery voltage will differ from the MPP voltage and thus the PV will deliver less energy than it could. This energy loss is indicated “No MPPT” in the Sankey diagrams shown later.

3.6 Wind turbines

The wind turbines models are based on power curves (electrical output power versus wind speed). It should be noted, however, that measurement of power curves for small wind turbines is notoriously difficult and field performance often falls short of manufacturer’s curves.

The curves also assume that the turbine rotational speed is well controlled to match the wind speed, which is not always the case.

3.7 Batteries

Charging and discharging losses are modelled according to manufacturer’s data at specified charge/discharge rates (C50, C100 etc.). This provides a state-of-charge estimate, which is used to determine cell voltage, again allowing for charge/discharge rate. Ambient temperature and battery ageing are not included in the model; these could be significant in the life of an ADU-RES system.

3.8 Power electronic converters (including inverters)

Losses in DC-DC converters and DC-AC inverters are a function of power flow (or current) and these are modelled based on manufacturer’s efficiency curves wherever possible. Additional losses in motors, generators and batteries due to harmonics caused by power electronic converters are not modelled but should be small provided that good-quality converters are used.

3.9 Induction motors

Efficiency curves for induction motors are based on actual manufacturer's data, supplemented by data for very similar motors manufactured by Brook Crompton[9]. Power factors of three-phase motors are similarly modelled as a function of operating power. Power factors of single-phase motors are harder to predict, because capacitor and winding arrangements differ between manufacturers. They were treated as constants between 0.96 and 0.98. Any errors have only a second-order effect on energy losses: reactive current will cause small losses in power electronic converters.

3.10 Centrifugal pumps

The efficiency of centrifugal pumps is critically dependent on operating point. This is modelled through application of the manufacturer's head-flow and power-flow curves. In some cases, data from very similar Grundfos pumps was substituted.

3.11 Positive displacement pumps

The geometric displacement, taken from the manufacturer's data, is used to calculate ideal flow and torque. Volumetric and mechanical efficiency curves are then applied to determine losses as a function of operation point.

3.12 DC motor-pumps

The DC motors in the selected systems are integrated with their respective pumps and were modelled using manufacturer's performance curves for the complete units.

3.13 Membranes

The models of the RO elements in the Matlab/Simulink model are derived from Dow FilmTec's ROSA[10].

3.14 Clark pump

The Clark pump model is based on detailed in-house measurements made over a broad range operation[11].

[9] www.brookcrompton.com
[10] http://www.dow.com/liquidseps/design/rosa.htm
[11] Thomson, Murray (2004). *Reverse-Osmosis Desalination of Seawater Powered by Photovoltaics Without Batteries*, PhD, University of Loughborough, UK. http://www-staff.lboro.ac.uk/~elmt/Thesis.htm Section 5.2

3.15 Filter and pipe losses

Pressure losses in filters and pipes are not included in the model. They are expected to be small, provided that filters are kept clean, pipe diameters are adequate, lengths are kept short and sharp elbows are avoided.

3.16 Flushing, cleaning, fouling and scaling

Flushing and cleaning directly affect the overall specific energy consumption in two ways:

- Energy is consumed by the pumps used during flushing and cleaning.
- Product water is consumed, reducing the overall system output.

All RO systems require flushing and cleaning (or have to accept very frequent membrane replacement), but quantifying this and the resulting decline in membrane performance is beyond the scope of the modelling presented here.

RO systems operating intermittently, with variable flow or at relatively low flows may be more prone to fouling than those operating at continuous high flow.

4 ITC DESSOL Seawater PV-RO, Gran Canaria

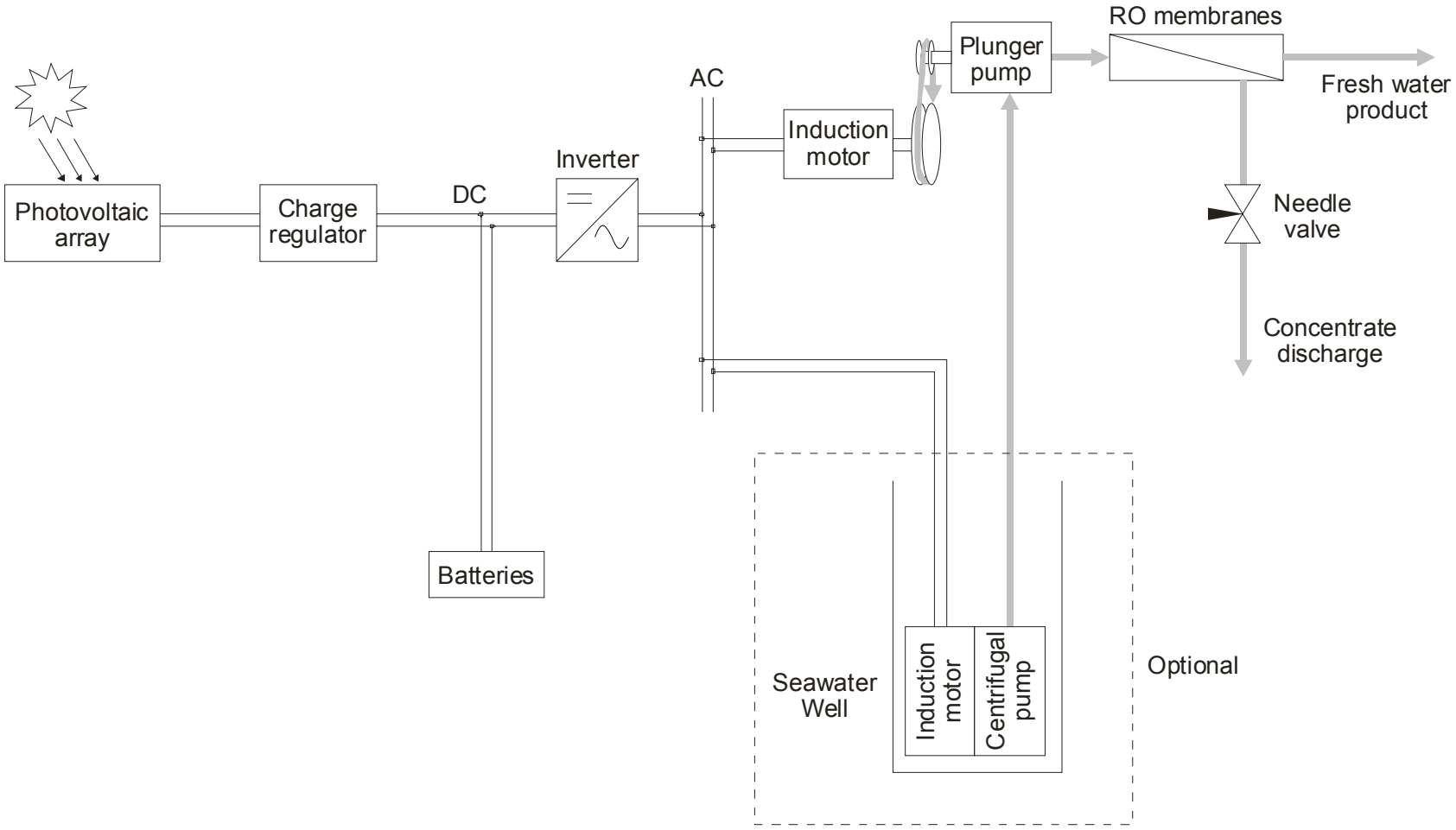

Figure 4 – General Arrangement – ITC DESSOL Seawater PV-RO, Gran Canaria

4.1 Assumed details

The details given here were used for the modelling described in this report and may differ from those of the actual installed system.

The model is based on the system operated by ITC, Pozo Izquierdo, Gran Canaria[12].

The actual system does not have the well pump shown in Figure 4; instead, it is fed by a general site supply of seawater, which is pumped using grid electricity. The centrifugal well pump shown in Figure 4 is the proposed supply method for an autonomous system. The modelling was completed both with and without this well pump.

RO operational parameters

Product flow	400 L/h
Recovery Ratio	45 %
Feed flow	900 L/h
Working pressure	55 bar

Seawater feed

Concentration	35 500 ppm TDS
…Osmotic pressure	26.3 bar
Temperature	19 °C to 23 °C

Solar radiation

Annual average:		
On a horizontal surface	5.6 kWh/m^2/d	
Inclined at 10 degrees	5.8 kWh/m^2/d	www.cabildodelanzarote.com/energias/gonzalopiernavieja.pdf - page 40
Hourly data	Meteonorm	http://www.meteotest.ch/
	And scaled to give an annual average of 5.8 kWh/m^2/d.	

Ambient temperature (for PV)

Hourly data	Meteonorm	http://www.meteotest.ch/

[12] ADU-RES, Work Package 2, Final Report, section 4.3.2.

Photovoltaic array

Nominal array power	4.8 kW_{peak}	
Number of modules	64	
Wiring configuration	16 strings each comprising 4 modules in series	
Nominal module power	75 W_{peak}	
Module type	Mono-crystalline	
Manufacturer	Atersa	www.atersa.com
Model	A-75	www.heliplast.cl/pdf/a75m.pdf
Cells per module	36 in series	
MPP voltage	17.0 V	

Batteries

Type	Flooded lead-acid	
Manufacturer	Fulmen Solar	
Capacity	400 Ah at 100 h rate	
Configuration	24 cells in series	
Nominal overall voltage	48 V	
Nominal energy capacity	19.2 kWh	
Assume performance details from:		
Manufacturer	BP Solar	www.bpsolar.com.au
Model	PVSTOR 2P430	http://www.bp.com/... /Aust_ps_solar_PVstorBrochure.pdf
Capacity	430 Ah at 100 h rate	www.solartech.com.au/pdfs/products/batteries/pv_stor_manual_5.pdf

Inverter

Manufacturer	Trace, Xantrex	www.xantrex.com
Model	SW4548E	SW Series Inverter/Chargers – (4.01 Software Revision) User Guide
Nominal Input	48 V, DC	http://www.xantrex.com/web/id/610/docserve.asp
Output	230 V, 50 Hz, Single-phase	
Rated power	4500 VA	
Efficiency (peak)	96 %	
Efficiency curve	From User Guide Figure 19	

Motor (for plunger pump)

Type	4-pole Single-phase induction	
Power	2.2 kW	
Assume other parameters similar to:		
Manufacturer	Brook Crompton	
Model	TDA100LZ (4-pole, low running current)	www.brookcrompton.com/pdf-files/2227e_1phase_v1.1e.pdf
Rated speed	1430 rpm	
Rated current	13.0 A	
Efficiencies	78 % at full load, 76 % at ¾ load, 71 % at half load	
Power factor	0.96 (assumed constant)	

Belt drive (for plunger pump)

Ratio	0.62	To give rated pump speed at rated motor speed.
Efficiency	97 % (assumed)	

Plunger pump

Manufacturer	CAT	www.catpumps.com
Model	317	http://www.catpumps.com/select/pdfs/317.pdf
Rated flow	15 L/m = 900 L/h	
Rated speed	950 rpm	

Volumetric and mechanical efficiency curves from CREST's own testing of a CAT 317.

RO membranes

Type	Spiral-wound, polyamide thin-film composite, for seawater	
Element size	2.5 inch by 40 inch	
Number of elements	12	
Configuration	2 parallel trains of 6 series elements	
Manufacturer	Dow FilmTec	http://www.dow.com/liquidseps/
Model	SW30-2540	http://www.dow.com/liquidseps/prod/sw30_2540.htm
Performance details	ROSA	http://www.dow.com/liquidseps/design/rosa.htm

Well pump (centrifugal)

As noted above, the well pump is the proposed supply method for an autonomous system. The demonstration system at ITC does not have its own well pump.

Rated pressure	3 bar	
Rated flow	2.5 m³/h	
Rated power	1 kW	
Depth (head)	4 m	
Manufacturer	Grundfos	www.grundfos.com
Model	CRT 2-5	Data booklet No.:V7149894, Grundfosliterature-942.pdf

Motor (for well pump)

Manufacturer	Grundfos	
Type	2-pole induction motor	
Rated (output) power	0.55 kW	
Full load efficiency	65 %	
Efficiency curve and other details based on:		
Manufacturer	Brook Crompton	www.brookcrompton.com/pdf-files/2227e_1phase_v1.1e.pdf
Model	2-TDA71MR (2-pole)	

4.2 The completed model

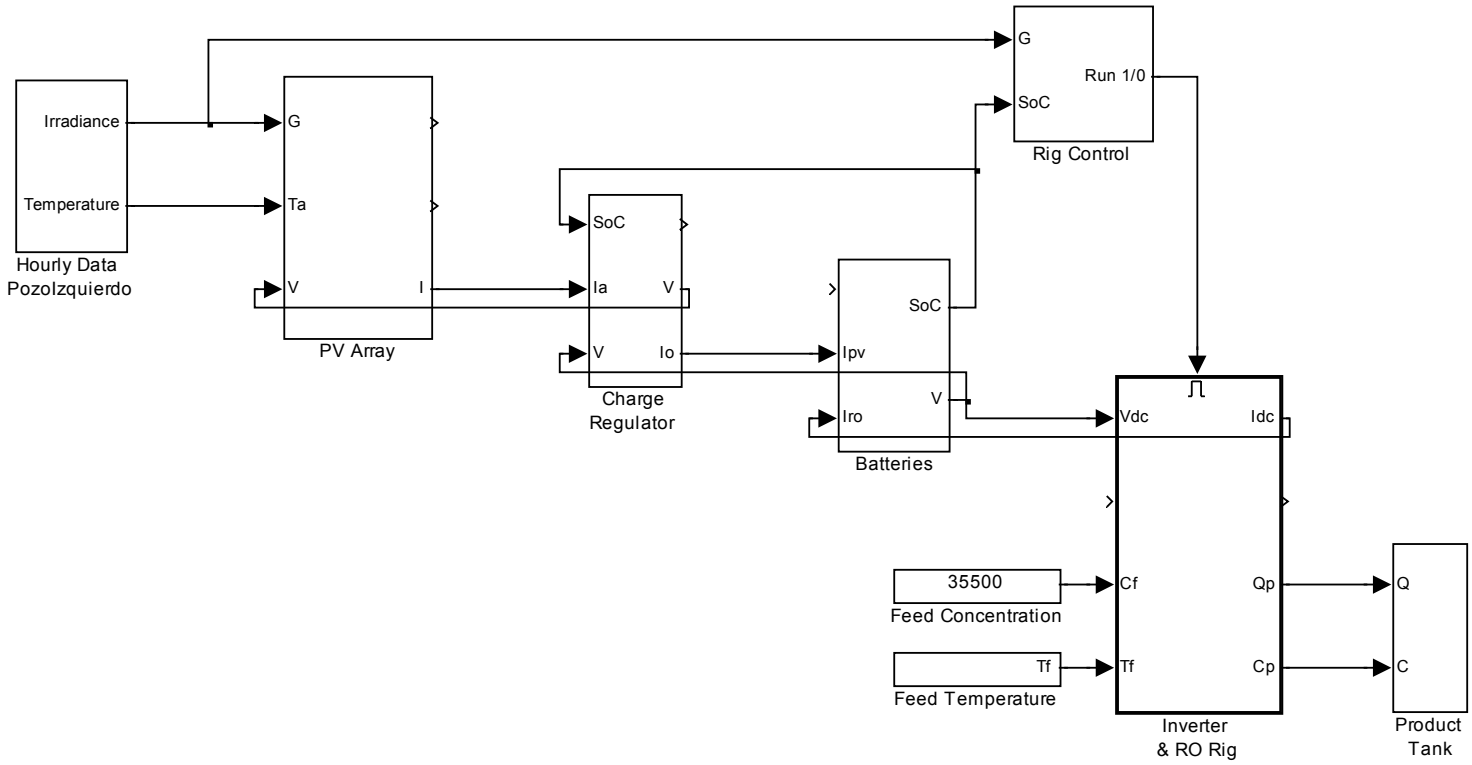

Figure 5 – Top level of Matlab-Simulink model of ITC DESSOL Seawater PV-RO

The data outlined in the previous section was used to construct a Matlab-Simulink model of the complete system using the approach outlined in Section 3. The model simulates one complete year of operation on an hour-by-hour basis. The model includes a controller that runs the RO rig according to the available solar radiation and the battery state of charge. Thus, the daily water

production varies according to the solar radiation data. The annual water production is logged and used to calculate annual average specific energies throughout the system.

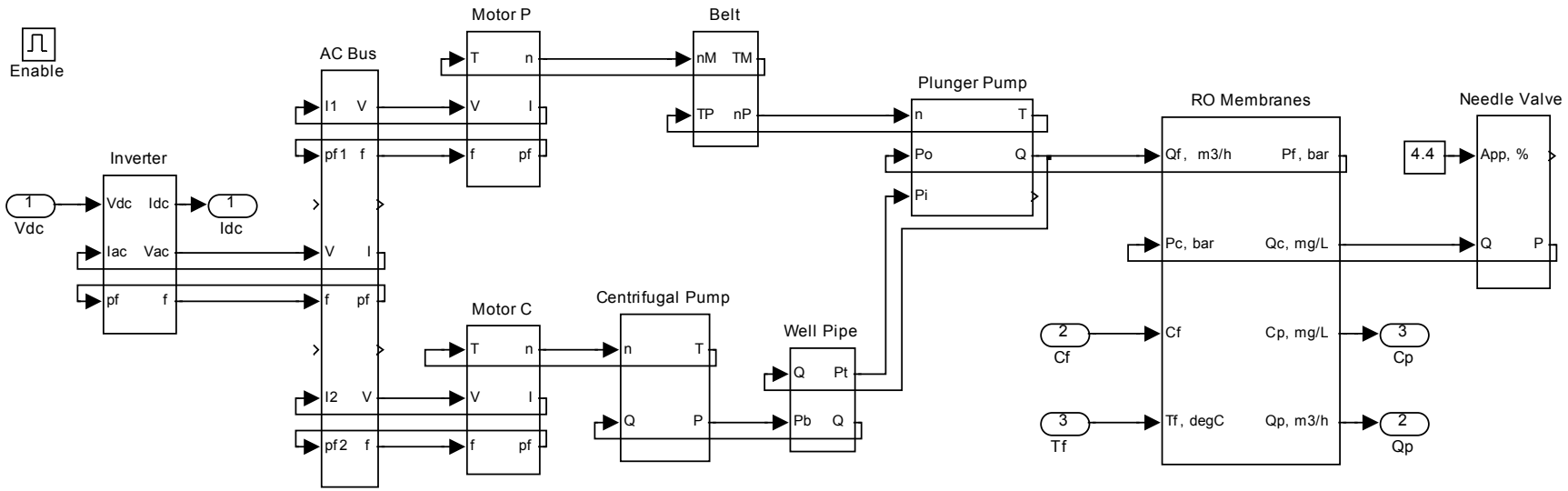

Figure 6 – Contents of the “Inverter and RO Rig” block shown in Figure 5

The individual component blocks shown in Figure 6 correspond to the hardware components shown earlier in Figure 4. The arrowed lines connecting the component blocks in Figure 6 represent the flows, pressures, voltages, currents, etc. in the respective pipes and wires of the real system. The arrows indicate the direction of the data flow, *not* the actual directions of water or current flow.

Notice that in many cases the arrowed lines carry the data backwards and thus form “algebraic loops”. This is a natural consequence of a physically interconnected system. Matlab-Simulink uses an iterative solver to perform such calculations.

The contents of the individual component blocks perform the detailed calculations according to the efficiency curves etc. outlined in the preceding section.

4.3 Modelled performance – without the well pump

General results from the model

Annual energy available from PV	8820 kWh/y
Annual hours run	2935 h/y
Average hours run per day	8.09 h/d
Annual water production	1200 m^3/y
Average daily water production	3.29 m^3/d
Overall annual average specific energy	8820/1200 = 7.35 kWh/m^3

The above figures, particularly the average hours run per day and the average daily water production show good agreement with the figures reported by ITC for the real demonstration system.

The overall specific energy figure shown above is calculated from the energy *available* from the PV. It is therefore higher that the figure of 5.5 kWh/m^3 measured by ITC at the input to the plunger pump motor (see also the following discussion).

Sankey diagram

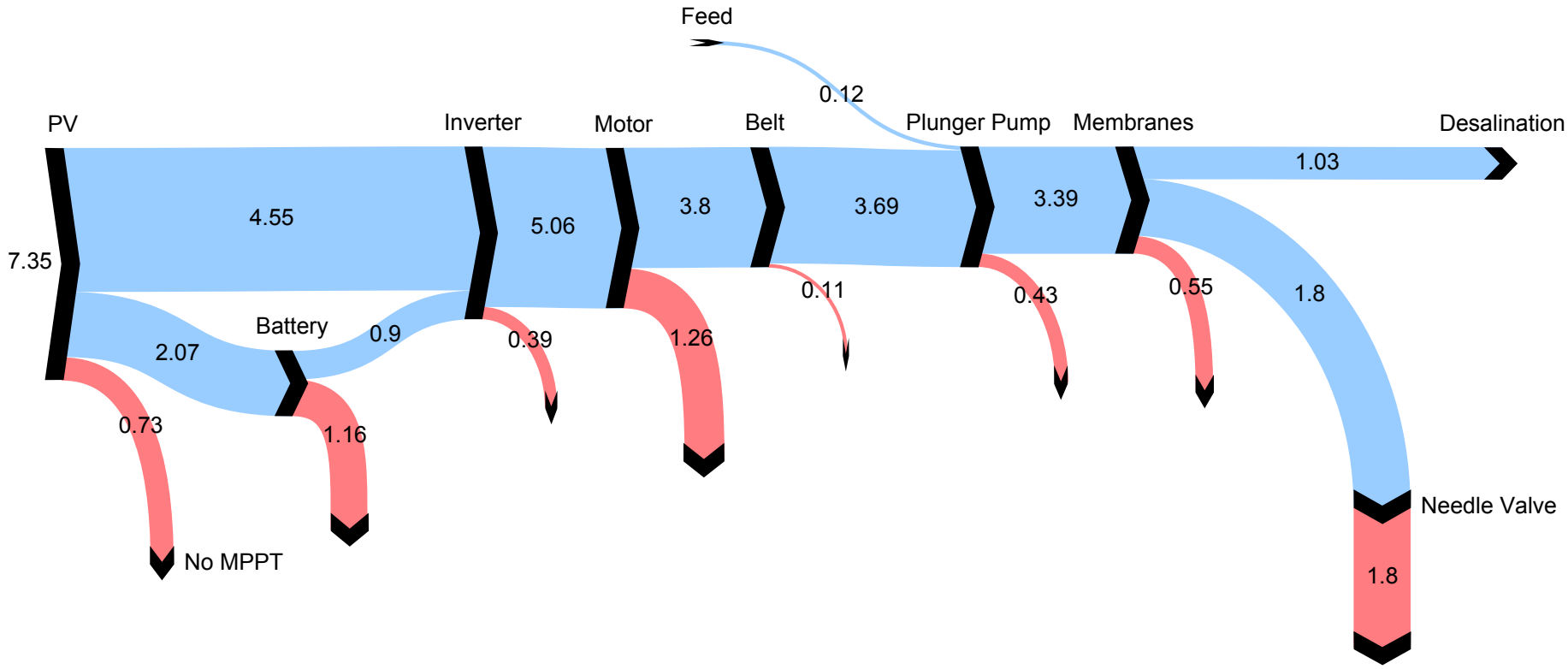

Figure 7 – Sankey diagram of energy flows in ITC DESSOL – without the well pump.
Line widths and numeric values represent annual average specific energies in kWh/m^3.

Discussion

The Sankey diagram of Figure 7 represents the modelled energy flows through the hardware components shown earlier in Figure 4.

The energy generally moves from left to right along the blue paths. The losses from the individual components are indicated in red.

Starting at the left, the width of the arrow labelled **PV** represents the total energy available from the PV array given the local solar radiation and ambient temperature conditions. Most of the energy goes directly to the inverter, some goes to the battery and some is lost because the system has no maximum power point tracking (**MPPT**). In the absence of MPPT, the voltage of the PV is determined by the battery and this will rarely coincide with the peak efficiency of the PV.

Next, we observe that the **battery** efficiency is rather low. The calculated figure was just 44 %, while manufacturer's figures for flooded lead-acid batteries are normally around 85 %. This is because the manufacturers quote battery efficiencies under slow-charge / slow-discharge conditions, for example over 100 hours, but the PV-RO system being modelled here can charge / discharge its batteries completely in less than 4 hours.

Thus, we see the importance of ensuring that the majority of the energy goes directly from the PV to the inverter. This is achieved by controlling the operational hours of the RO rig to coincide closely with the available solar energy. In the real demonstration system, the **on/off control** of the RO rig is computer controlled, taking into account the time of day and an estimate of the battery state of charge. The model employs a slightly different algorithm based on the solar radiation and the state of charge, but achieves a very similar average run time of around 8 hours per day.

The **inverter** efficiency is around 93 %, modelled according to the manufacturer's efficiency curve, and assuming that the inverter is switched off when the rig is off. If, on the other hand, the inverter has to be left running (in order to supply control systems for example) it will be slightly less efficient overall.

The model shows that the **motor** operates at 75 % efficiency, and the resulting energy loss exceeds that of the battery. There are several factors contributing to the motor's efficiency:

- It is a small motor, rated at 2.2 kW. Larger motors are significantly more efficient.
- It is an induction motor. Permanent magnet motors can offer better efficiency, but are much more expensive and less widely available.
- It is a single-phase motor, presumably because the inverter is single-phase. Three-phase induction motors are generally more efficient.
- The model assumes it is a “standard-efficiency” motor. Most manufacturers now offer “high-efficiency” motors (particularly in three-phase) that are significantly better.
- The motor is running at 69 % of its rated output, which is not the best efficiency point of the motor chosen for the model.

The model includes a drive **belt** to match the motor speed to that required by the plunger pump. The belt efficiency is assumed to be 97 %, which is perhaps optimistic.

Two energy flows enter the **plunger pump**: the main one is the shaft power from the belt; the other is from the pressure of the seawater feed, which, as noted earlier, is from a general site supply pumped using grid electricity. The model assumes the pressure of this feed is 2 bar, and shows that, at this pressure, its energy contribution is minimal.

The efficiency of the plunger pump itself is very good: something over 88 %, according to CREST’s testing of a pump of the exact same model. Note that this is the overall energy efficiency, including both volumetric and mechanical efficiencies.

The indicated **membrane** losses include both through-flow and cross-flow losses, as discussed in section 2.4. These losses could be reduced by operating at a lower membrane feed pressure, for example by opening the needle valve slightly. But, this would also reduce the flow of product water and, *in the absence of brine-stream energy recovery*, this would cause an increase in specific energy at the membranes feed, and throughout the system.

The largest energy loss in the system is in the **needle valve**, which wastes all of the hydraulic energy available in the concentrate. A brine-stream energy recovery mechanism would return some (hopefully most) of this energy to the system and thus reduce

overall energy consumption. Notice however that this system has a water recovery ratio of 45 %, which is quite high for small-scale seawater RO. Thus, the energy available in the concentrate is proportionally less than in some other seawater systems and the need for energy recovery is not so great.

The 1.03 kWh/m^3 attributed to **desalination** at the right of the Sankey diagram represents the theoretical minimum energy required to desalinate seawater at 45 % recovery ratio, as illustrated in Figure 1.

Overall, we see that the specific energy consumption measured at the input to the motor is 5.06 kWh/m^3, according to the model. This compares well with the figure of 5.5 kWh/m^3 measured by ITC on the real system. Either figure is very commendable for such a small-scale seawater RO system without energy recovery.

The efficiency of the **single-phase induction motor** is only 75 % (assuming the data used for the modelling is accurate). A small reduction in specific energy consumption could perhaps be achieved by using a different type of motor, but to achieve significant improvement, the system would have to be larger. For example, doubling the system size would allow use of a 4 kW three-phase motor providing 87.5 % efficiency.

The efficiency of the **batteries** is also rather low: just 44 % according to the model. The basic problem is the rapid discharge rates which result form the battery capacity (400 Ah) being small in relation to the discharge currents (up to 45 A in the model).

The lack of maximum power point tracking (MPPT) also leads to significant loss of available energy, but adding MPPT to a battery-based system requires an extra power-electronic converter, which is expensive and incurs its own energy losses. The model shows that some improvement could be made by better matching of the battery voltage (number of cells) to the MPP voltage of the PV array. The modelled MPP voltage, however, relies upon a simple NOCT calculation of the PV module temperature. Local conditions, particularly wind, could alter this result significantly.

4.4 Modelled performance – including the well pump

General results from the model

Annual energy available from PV	8820 kWh/y
Annual hours run	2357 h/y
Average hours run per day	6.46 h/d
Annual water production	960 m^3/y
Average daily water production	2.63 m^3/d
Overall annual average specific energy	8820/960 = 9.19 kWh/m^3

The annual energy available from the PV (8820 kWh/y) is unaffected by the addition of the well pump to the model. But, a considerable proportion of this energy is now used by the well pump, and so the annual water production predicted by the model is reduced from 1200 m^3/y to 960 m^3/y. This is reflected in the substantial increase in the overall specific energy, from 7.35 kWh/m^3 to 9.19 kWh/m^3.

Sankey diagram

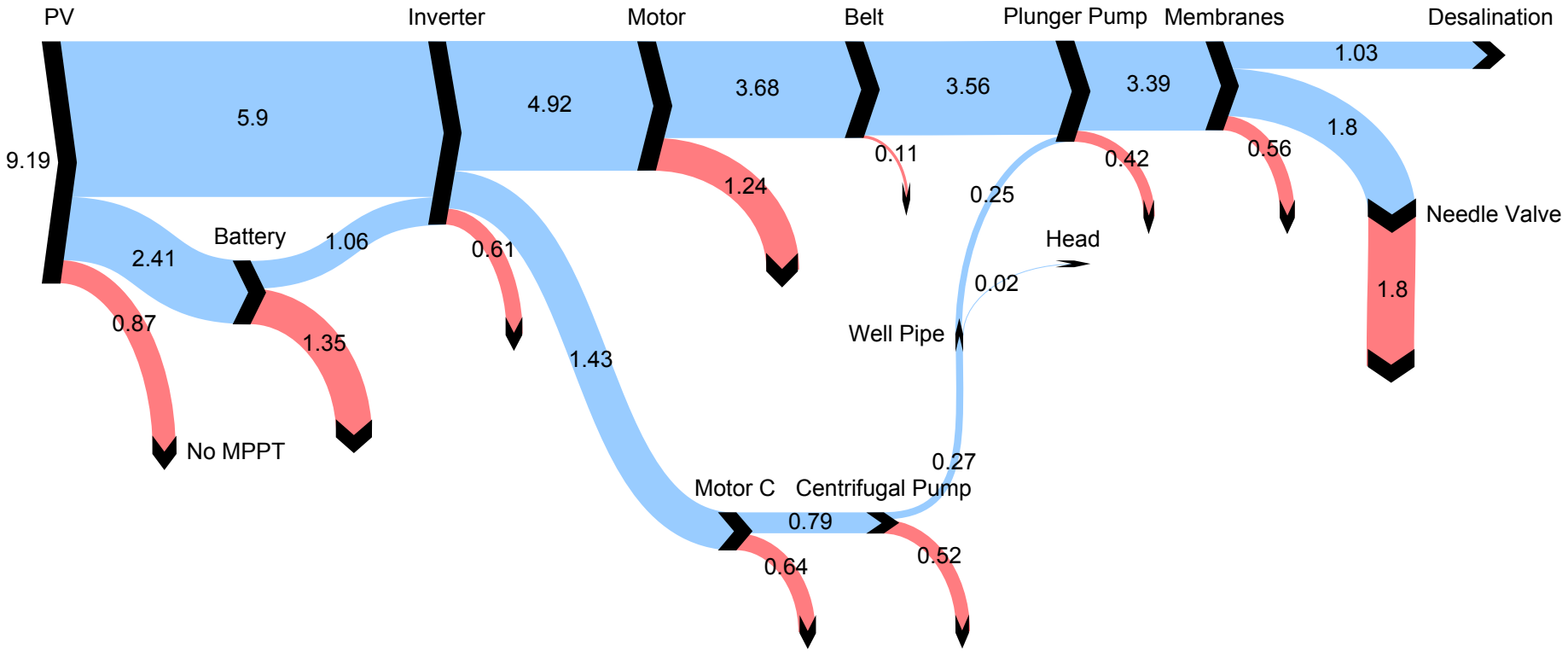

Figure 8 – Sankey diagram of energy flows in ITC DESSOL – including the well pump.
Line widths and numeric values represent annual average specific energies in kWh/m^3.

Discussion

The proposed well pump is rather inefficient. It is a small centrifugal pump, operated well away form its best-efficiency point, driven by a small single-phase induction motor, also operated away form its best-efficiency point.

The well pump's main task is to lift the water just 4 metres; this head corresponds to just 0.02 kWh/m^3, whereas the electricity consumed by the well-pump motor is 1.43 kWh/m^3. A small proportion of the energy (0.25 kWh/m^3) is passed to the plunger pump, and will serve to slightly reduce the load on its motor, but the rest of energy is simply lost.

The proposed well pump illustrates how seemingly small devices can have a significant effect on overall energy efficiency.

On the other hand, the well pump plays an important role, not only lifting the water, but also pushing it through the pre-filters and preventing cavitation in the plunger pump. Furthermore, centrifugal pumps are generally very reliable and require minimal maintenance. Finding a suitable alternative pump is not at all straightforward.

One suggestion is to use a much bigger pump to quickly fill a header tank. Being larger would greatly improve the pump and motor efficiencies. Moreover, having a header tank would allow the two motors to run independently, and this could be exploited by the controller so as to reduce the energy going through the batteries, which would bring a further significant energy saving.

5 CRES Seawater PV-Wind-RO, Lavrio, Greece

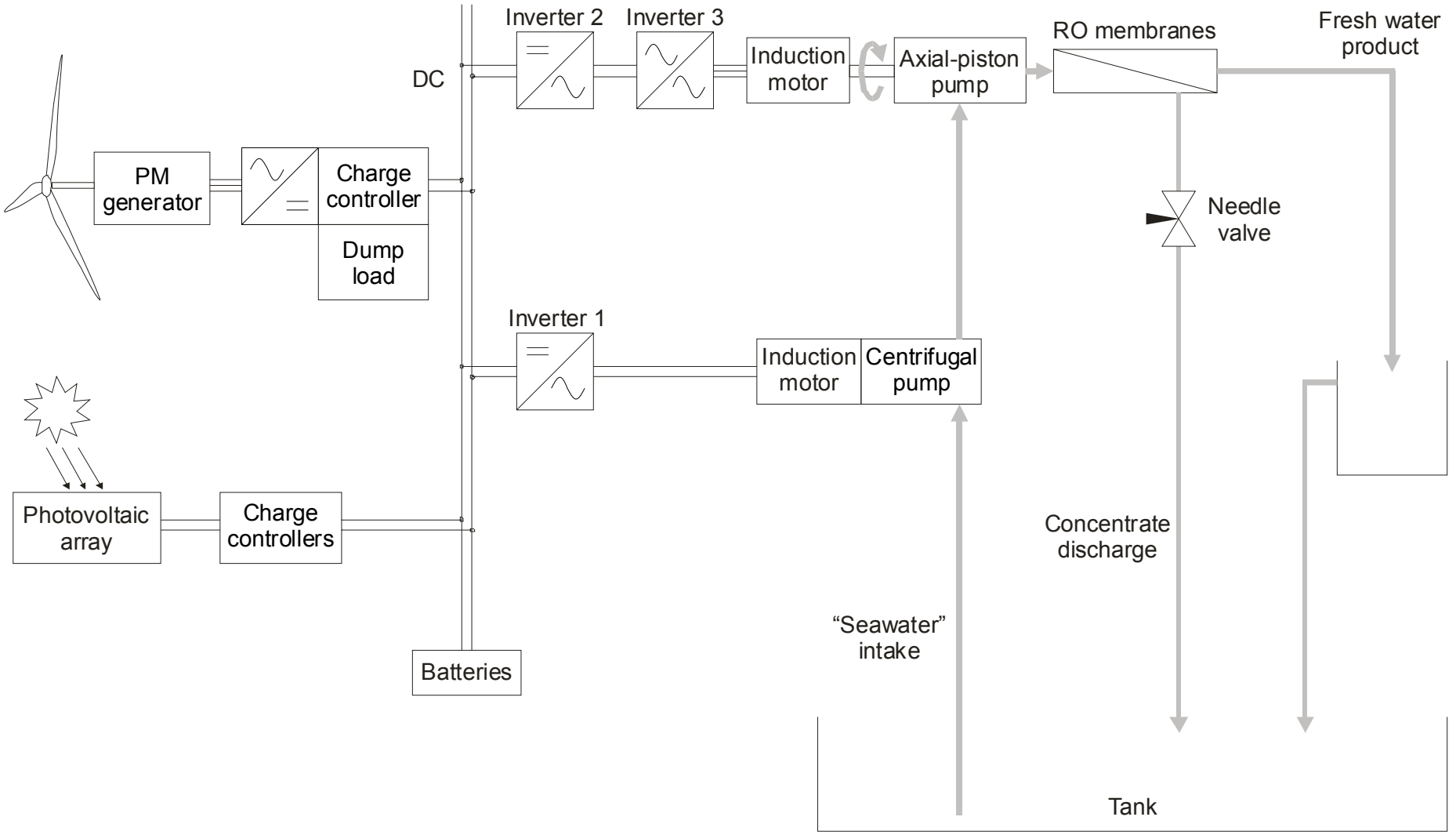

Figure 9 – General Arrangement – CRES Seawater PV-Wind-RO, Lavrio, Greece

5.1 Assumed details

The details given here were used for the modelling described in this report and may differ from those of the actual installed system.

The model is based on the **new** system operated by CRES at Lavrio, Greece, since December 2004[13]. The earlier version of the system used the same energy supply components[14].

RO operational parameters

Product flow	150 L/h
Recovery Ratio	13 %
…Feed flow	1154 L/h = 19.23 L/m

Feed water

Concentration	37 000 ppm TDS seawater equivalent NaCl
…Osmotic pressure	~ 27.4 bar
Feed temperature	25 °C

Solar radiation

Hourly data	Meteonorm for Lavrio, Greece	http://www.meteotest.ch/
Inclination	Equal to latitude	
Annual average	4.7 kWh/m^2/d	4.7x1000/24
Compares well with:		
Annual average horizontal	4.52 kWh/m^2/d	http://re.jrc.cec.eu.int/pvgis/pv/countries/europe/g13y_gr.png

Ambient temperature (for PV)

Hourly data	Meteonorm	http://www.meteotest.ch/

[13] ADU-RES, Work Package 2, Final Report, section 4.5.1, page 88.
[14] Tzen, Eftihia, D. Theofilloyianakos, M. Sigalas and K. Karamanisc (2004). Design and development of a hybrid autonomous system for seawater desalination. *Desalination* **166**: 267-274

Wind speed

Annual average	6.7 m/s	Sounding Techniques in Wind Energy Applications, Mouzakis et al.
Assume hub height equals measurement height		
Hourly data	Measured at RAL, Oxfordshire, UK, and scaled to give an annual average of 6.7 m/s.	

Photovoltaic array

Nominal array power	3.96 kW_{peak}	
Number of modules	36	
Wiring configuration	3 sub-arrays each comprising 12 modules in parallel	
Nominal module power	110 W_{peak}	
Module type	Mono-crystalline	
Manufacturer	Siemens (Then Shell, then Solar World, now discontinued.)	
Model	SM110	http://www.a1solar.co.uk/sm110_sm100.html
Cells per module	72 in series	
Nominal module voltage	24 V	
MPP voltage	35.0 V	
I-V curve details from:		
Manufacturer	Shell	
Model	SM110-24P	http://www.wind-sun.com/PDF_Files/ShellSM110-24P_USv1.pdf

Charge controllers (for PV)

Quantity	3, one for each sub-array	
Manufacturer	Steca	www.stecasolar.com
Model	Tarom 245	www.solardome.co.za/Pdf/Steca%20Tarom.pdf
Type	Shunt PWM	http://www.solarlink.de/PDF-Files/Steca/TAROM_Emanual.pdf
MPPT	No	

Wind turbine

Manufacturer	Southwest Windpower	www.windenergy.com
Model	Whisper H40	www.windenergy.com/Whisper500Manual.pdf
Power	460 W at 10 m/s (rated)	
	900 W at 12.5 m/s (peak)	
Generator	Permanent magnet	
	Variable frequency	
	3-phase	
Nominal voltage	24 V AC	
Rectifier/controller	EZ-Wire 120/1600	www.windenergy.com/Whisper500Manual.pdf
	Diode bridge rectifier	
	Dump load controlled on battery voltage	
Power curve	NREL, Power Performance Test Report	www.nrel.gov/wind/pdfs/32748.pdf
	Table 3. DC Power Performance at Sea-Level Air Density	

Batteries

Type	Flooded lead-acid	
Manufacturer	Fulmen Solar	
Capacity	1850 Ah at 100 h rate	
Configuration	12 cells in series	
Nominal overall voltage	24 V	
Assume performance details from:		
Manufacturer	BP Solar	www.bpsolar.com.au
Model	PVSTOR 2P1110	http://www.bp.com/... /Aust_ps_solar_PVstorBrochure.pdf
Capacity	1110 Ah at 100 h rate	www.solartech.com.au/pdfs/products/batteries/pv_stor_manual_5.pdf
	But scaled to give 1850 Ah at 100 h rate.	

Inverter 1 (for centrifugal pump)

Manufacturer	Siemens	
Model	ESW 3024	http://www.photovoltaic.gr/inverters/english.htm
Nominal Input	24 V DC	
Output	230 V AC, 50 Hz, Single-phase	

Assume efficiency curve from:

Manufacturer	Trace, Xantrex	www.xantrex.com
Model	SW3024E	SW Series Inverter/Chargers – (4.01 Software Revision) User Guide
Peak Efficiency	94 %	http://www.xantrex.com/web/id/610/docserve.asp
Typical Efficiency	91 %	

Centrifugal pump

Type	2-stage centrifugal	
Manufacturer	Lowara	
Model	2HMS3/A	http://www.lowara.com/pdf/en/hmhmsxxxxx-bx.pdf
Flow-pressure data	Hydraulic Performance Table, HMS Series, page 6	

Assume power curve from:

Manufacturer	Grundfoss	www.grundfos.com
Model	CHI 2-20	Data booklet No.:V7031261, Grundfosliterature-1117.pdf

Motor for centrifugal pump

Manufacturer	(Lowara)	
Type	2-pole single-phase induction motor	http://www.lowara.com/pdf/en/hmhmsxxxxx-bx.pdf
Power	0.3 kW	
Model	SM63HM/1035	
Frame size	63	
Voltage	220-240 V, 50 Hz	
Full-load current	2.25 A	
Full-load efficiency	300/230x2.25x0.97 = 60 %	

Assume other parameters similar to:

Manufacturer	Brook Crompton Single phase motors	www.brookcrompton.com/pdf-files/2227e_1phase_v1.1e.pdf
Power factor	0.97	
Part-load efficiencies	58 % at ¾ load, 52 % at half load	

Inverter 2 (for AP pump)

Manufacturer	Respect
Nominal Input	24 V, DC

Output	230 V AC, 50 Hz, Single-phase	
Continuous rating	3000 VA	

Assume efficiency curve from: Trace, Xantrex, SW3024E, as per Inverter 1.

Inverter 3 (also for AP pump)

Type	Variable frequency drive (VFD)	
Manufacturer	LG Industrial Systems	www.lgis.com
Range	Starvert-iC5	www.anadigi.co.za/documents/iC5/iC5.pdf
Model	SV022iC5-1	
Rating	2.2 kW	

Assume loss-current curve from:

Manufacturer	FKI Industrial Drives	
Model	FID1000 FKI-12150	

Motor (for AP pump)

Type	Three-phase induction	
Manufacturer	Valiadis	
Model	Ê90L	http://www.valiadis.gr/en/motors/2pmotorsen.htm
Power	2.2 kW	
Frequency	50 Hz	
Rated speed	2850 rpm	
Efficiency	79 %	
Cos φ at full load	0.85	

Assume other parameters similar to:

Manufacturer	Brook Crompton	
Model	T-DA(DF)90LA	www.brookcrompton.com/pdf-files/2210E_issue3_1e.pdf

Axial-piston pump

Manufacturer	Danfoss	http://nessie.danfoss.com/products/pumps.asp
Model	APP 1.0	APP datasheet no.: DKCFN.PD.010.D4.02
Geometric displacement	6.3 cm^3/rev	
Volumetric efficiency	95 %	

Assume mechanical efficiency similar to:

Model	PAH 6.3	APP datasheet no.: DKCFN.PD.010.A6.02
Overall efficiency	77 % at 60 bar	
…Mechanical efficiency	81 %	

RO membranes

Type	Spiral-wound, polyamide thin-film composite, for seawater	
Element size	2.5 inch by 40 inch	
Number of elements	2	
Configuration	2 in series	
Manufacturer	Dow FilmTec	http://www.dow.com/liquidseps/
Model	SW30-2540	http://www.dow.com/liquidseps/prod/sw30_2540.htm
Performance details	ROSA	http://www.dow.com/liquidseps/design/rosa.htm

5.2 Modelled performance

General results from the model

Annual energy from wind turbine	1791 kWh/y
Annual energy available from PV	6305 kWh/y
Annual hours run	1430 h/y
Average hours run per day	3.92 h/d
Annual water production	217 m^3/y
Average daily water production	0.60 m^3/d
Overall annual average specific energy	(1791+6305) / 217 = 37 kWh/m^3

Sankey diagram

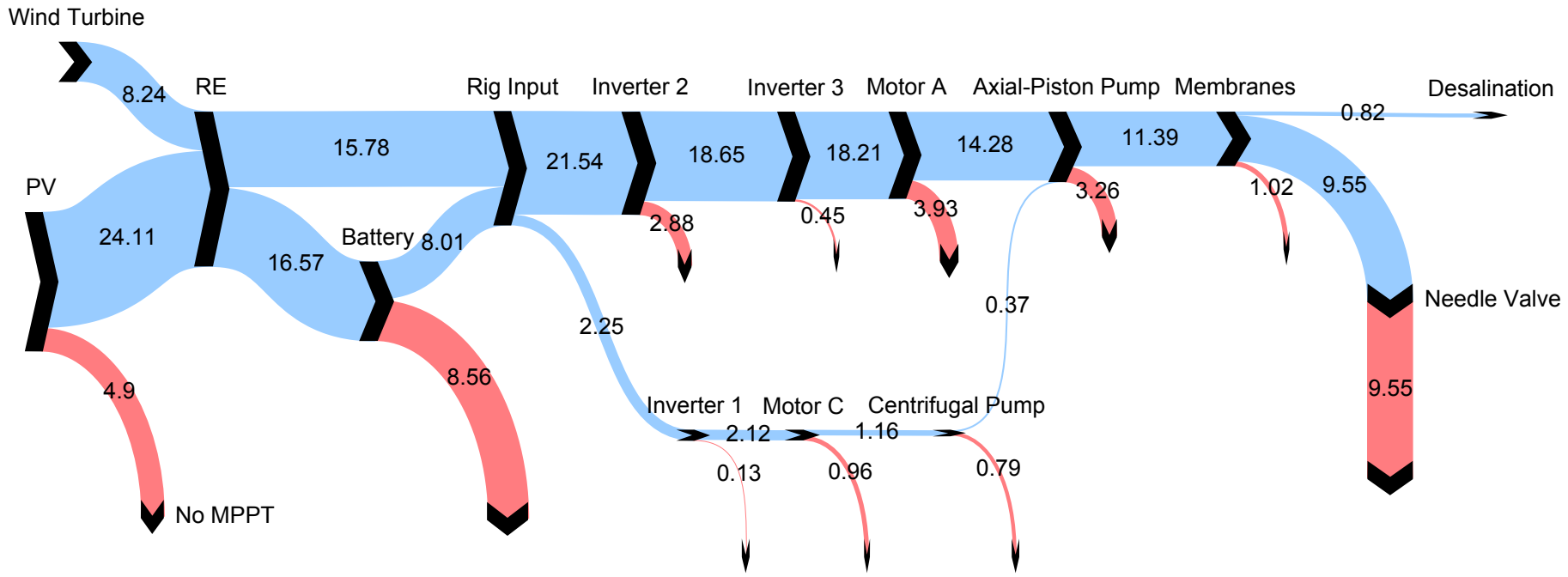

Figure 10 – Sankey Diagram – CRES Seawater PV-Wind-RO, Lavrio, Greece.
Line widths and numeric values represent annual average specific energies in kWh/m^3.

Discussion

The Sankey diagram of Figure 10 represents the modelled energy flows through the hardware components shown earlier in Figure 9.

The energy generally moves from left to right along the blue paths. The losses from the individual components are indicated in red.

Starting at the left of Figure 10, we see that roughly three quarters of the energy is coming from the **PV,** with the remainder from the **wind turbine**. The exact proportions of wind and PV energy depend critically on the wind speed and solar irradiance data used in the model, and could be significantly different in practice. Furthermore, the annual average data shown in the Sankey diagram does not indicate seasonal variations; for example, the wind turbine could be playing an important role during a season of low solar irradiance.

The width of the arrow labelled **PV** represents the total energy available from the PV array given the local solar irradiance and ambient temperature conditions. Part of this energy is lost because the system has no maximum power point tracking (**MPPT**). In the absence of MPPT, the voltage of the PV is determined by the battery and this will rarely coincide with the peak efficiency of the PV. According to the model, this energy loss is approximately 20 % of the total energy available from the PV array. Looking back to Figure 7, we see the MPPT losses in ITC DESSOL were only 10 %; the difference is due to the matching of the battery voltage to the MPP voltage in the two systems. However, these calculated losses depend on a simple NOCT calculation of the PV module temperature. Local conditions, particularly wind, could alter the results significantly. Nonetheless, the point is that battery and MPP voltages must be carefully matched in order to avoid very significant energy losses in systems without MPPT.

Next, we observe that the modelled **battery** efficiency is 48 %. This is slightly better than the 44 % shown by the ITC DESSOL model, but still nowhere near manufacturer's figures of around 85 %. Again, the low battery efficiency is due to the very high charge / discharge rates in the PV-RO system. The figure for Lavrio is slightly better than DESSOL, because the batteries are larger and the relative rates slightly reduced. But, the overall effect is significantly worse, because a much greater proportion of the energy is going through the batteries at Lavrio than in DESSOL. This is due to the relative sizes of the renewable-energy and RO rigs in the two systems.

Lavrio has three **inverters**: two for converting the battery DC to single-phase AC, and a third to convert single-phase to three-phase. The third inverter is an industrial variable frequency drive (VFD), also known as a frequency converter; it includes a diode-bridge rectifier to convert to DC prior to its main inverter stage, which converts back to AC. The multiple conversion through the inverters 2 and 3 in series causes multiple energy losses, which is not ideal, but closer inspection of the Sankey diagram shows

that the losses from inverter 3 are much less than from inverter 2. Inverter 2 is less efficient because it includes components to step up the voltage and smooth the output waveform.

The main **motor** in the Lavrio system achieves a slightly better efficiency than that in DESSOL, mainly because it is three-phase. This improvement in motor efficiency offsets some of the energy loss in inverter 3, which converts from single to three-phase.

The combined efficiency of the **centrifugal pump**, its motor and inverter is only 16 %. As with the DESSOL well pump, the main cause is the small size.

Two energy flows enter the **axial-piston pump**: the main one is the shaft power from the motor; the other is due to the pressure from the centrifugal pump. The losses from the axial-piston pump include both volumetric and mechanical efficiencies, the latter being assumed from a Danfoss PAH axial-piston pump, as opposed to the APP in use. With this assumption, the overall energy efficiency appears to be rather less than might be expected from a CAT plunger pump. On the other hand, the Danfoss axial-piston pump may require less maintenance.

The indicated **membrane** losses include both through-flow and cross-flow losses, see section 2.4. As discussed for DESSOL, there is little scope to reduce these losses.

Unsurprisingly, the largest energy loss in the system is in the **needle valve**. This was also the case with DESSOL, but with Lavrio an even greater proportion is lost, because it has a much lower water recovery ratio: 13 % as opposed to 45 %. Lavrio has just two membranes in series while DESSOL has six. The water exiting the second membrane element in Lavrio is passed directly to the needle valve; in DESSOL it goes through another four membrane elements, thus yielding a lot more product water and dramatically reducing the specific energy consumption. Thus, it may be useful to consider adding extra membrane elements at Lavrio. The alternative is to add brine-stream energy recovery, in which case the water recovery ratio becomes much less important.

6 CREST Seawater PV-RO

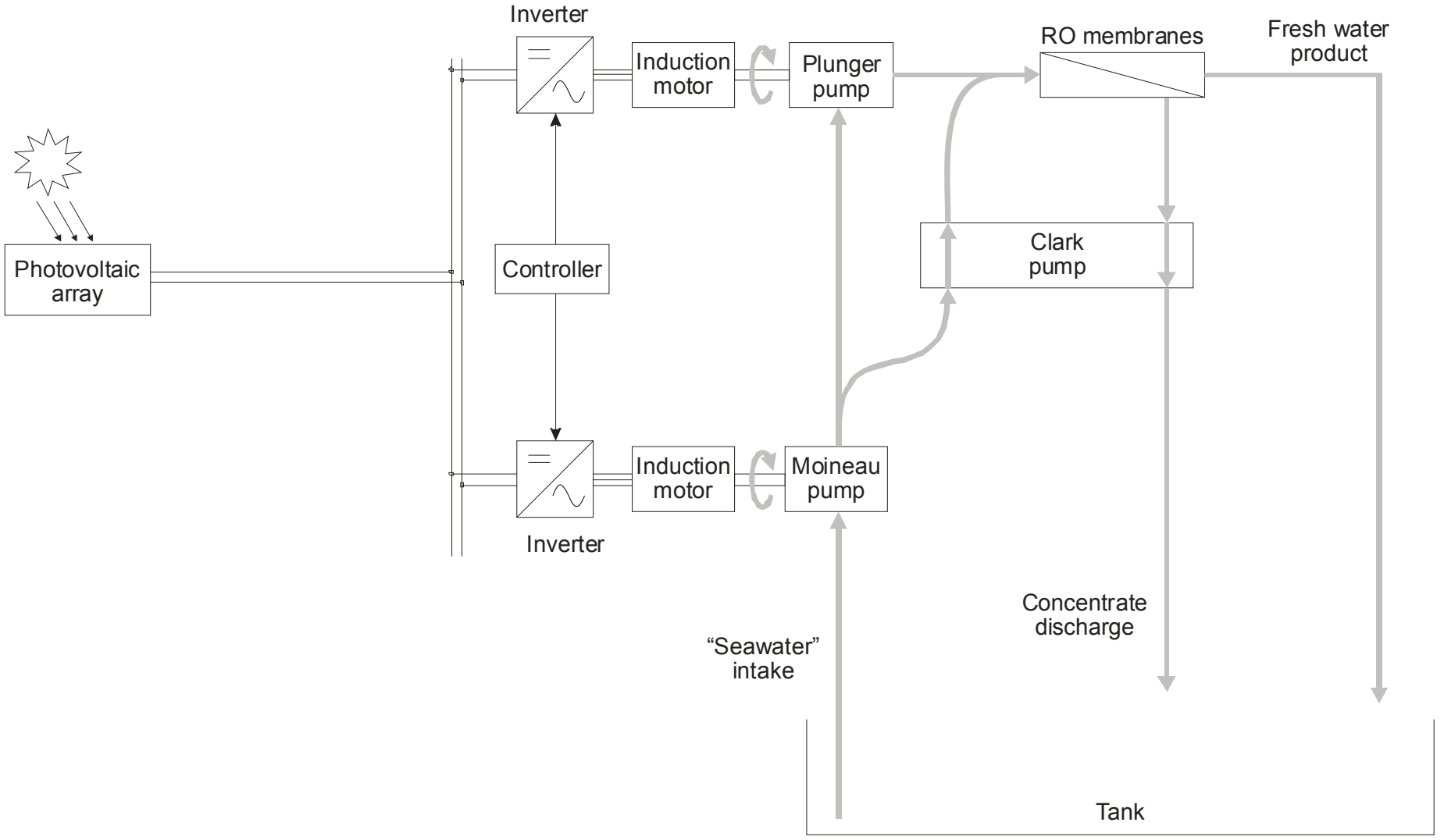

Figure 11 – General Arrangement – CREST Seawater PV -RO

6.1 System details

The CREST seawater PV-RO system[15] has no batteries. Its operation was demonstrated in Loughborough, UK, for two days in 2003. Loughborough is far from the sea, has no shortage of fresh water and has only a modest solar resource. The modelling presented here assumes that the system is operating in a more appropriate location, in particular Eritrea. Also, it is equipped with a 2.4 kW_{peak} PV array and two 6-pole motors; these details were different in the Loughborough demonstration.

RO operational parameters

Product flow	33 L/h to 460 L/h
Recovery Ratio	10 % to 38 %
Feed flow	330 L/h to 1280 L/h

Feed water

Composition	Straight NaCl solution
Concentration	35 000 mg/L, which is isosmotic with seawater at around 38,000 mg/L.
…Osmotic pressure	~ 28 bar
Feed temperature	17 °C to 33 °C

Solar radiation

Hourly data	Meteonorm for Massawa, Eritrea	http://www.meteotest.ch/
Inclination	17° with single-axis solar-trajectory tracking	
Annual average	7.8 $kWh/m^2/d$	

Ambient temperature (for PV)

Hourly data	Meteonorm for Massawa, Eritrea	http://www.meteotest.ch/

[15] Thomson, Murray (2004). *Reverse-Osmosis Desalination of Seawater Powered by Photovoltaics Without Batteries*, PhD, University of Loughborough, UK. http://www-staff.lboro.ac.uk/~elmt/Thesis.htm

Photovoltaic array

Nominal array power	2.4 kW_{peak}	
Number of modules	20	
Wiring configuration	20 in series	
Nominal module power	120 W_{peak}	
Module type	Poly-crystalline	
Manufacturer	AstroPower (now GE Energy)	www.gepower.com
Model	AP-1206	http://www.oksolar.com/pdf/solar_energy_catalog/astro-power_ap120.pdf
Cells per module	36 in series	
MPP voltage	16.9 V	

Inverters (both)

Type	Variable frequency drive (VFD)	
Manufacturer	FKI Industrial Drives (see Invertek)	www.invertek.co.uk
Model	FID1000 FKI-12150	
Rating	1.5 kW	
Nominal Input	230 V single-phase AC	
… or in this case	325 V DC	
Output	Variable frequency three-phase AC. Nominal: 230 V at 50 Hz.	
Losses	14.5 W at 1.3 A motor current	
	28.5 W at 3.4 A motor current	

Motors (both)

Type	6-pole three-phase high-efficiency induction motor
Power	1.5 kW
Manufacturer	Toshiba
Model	B0026FLF2AYH
Full-load efficiency	85 % IEC (based on IEEE 88.4 %)
European alternative:	
Manufacturer	Siemens
Model	1LA9 106-6KA
Full-load efficiency	83.0 % IEC (88.4 % IEEE)

Plunger pump

Manufacturer	CAT	www.catpumps.com
Model	237	http://www.catpumps.com/select/pdfs/237.pdf
Rated flow	8.7 L/m	
Rated speed	1725 rpm	

Volumetric and mechanical efficiency curves from CREST's own testing of a CAT 317.

Moineau pump

Manufacturer	Netzsch	www.netzsch-pumps.com
Model	NM021SY	

Efficiencies from manufacturer's performance curves.

Clark pump

Manufacturer	Spectra Watermakers Inc.	www.spectrawatermakers.com
Ratio	10 %	

Efficiency details from in-house testing at CREST[16]

RO membranes

Type	Spiral-wound, polyamide thin-film composite, high-flow for seawater	
Element size	4 inch by 40 inch	
Number of elements	4	
Configuration	4 in series	
Manufacturer	Koch	www.kochmembrane.com
Model	TFC1820HF	http://www.kochmembrane.com/pdf/8182001spiral.pdf
Performance details	RoPro (Koch software) plus in-house testing at CREST	

[16] *Theory, testing and modelling of a Clark pump*, Murray Thomson and Marcos Miranda, http://www.spectrawatermakers.com/articles/CREST_Clark_Pump.pdf

6.2 Modelled performance

General results from the model

Annual energy available from PV	5713 kWh/y
Annual hours run	4074 h/y
Average hours run per day	11 h/d
Annual water production	1424 m^3/y
Average daily water production	3.9 m^3/d
Overall annual average specific energy	5713/1424 = 4.01 kWh/m^3

The model shows that, if located in Eritrea, the CREST PV-RO system would run for an average of 11 hours per day. This high figure is primarily because the system runs at variable flow and hence with variable input power. To achieve its full output, the system needs up to 1600 W of DC power from the PV. But it can start and run, albeit slowly, with as little as 100 W. This was demonstrated with the test rig in Loughborough, operating directly from PV. The high solar resource in Eritrea and the proposed solar-trajectory tracking of the PV array also contribute to the 11 hours per day.

The model shows an overall annual average specific energy of just over 4 kWh/m^3. This low figure is mainly because:

- The system is fitted with brine-stream energy recovery, in the form of a Clark pump.
- The system has no batteries.

Other factors include:

- The use of maximum-power-point tracking (MPPT).

- Series connection of the PV array, giving a high DC voltage, which makes for efficiency in the inverters.
- Careful selection of the motors and pumps.
- A large membrane area.

On the other hand, the reliability of the system remains unproven. In particular, the low and variable flow rates may cause rapid fouling of the membranes.

Sankey diagram

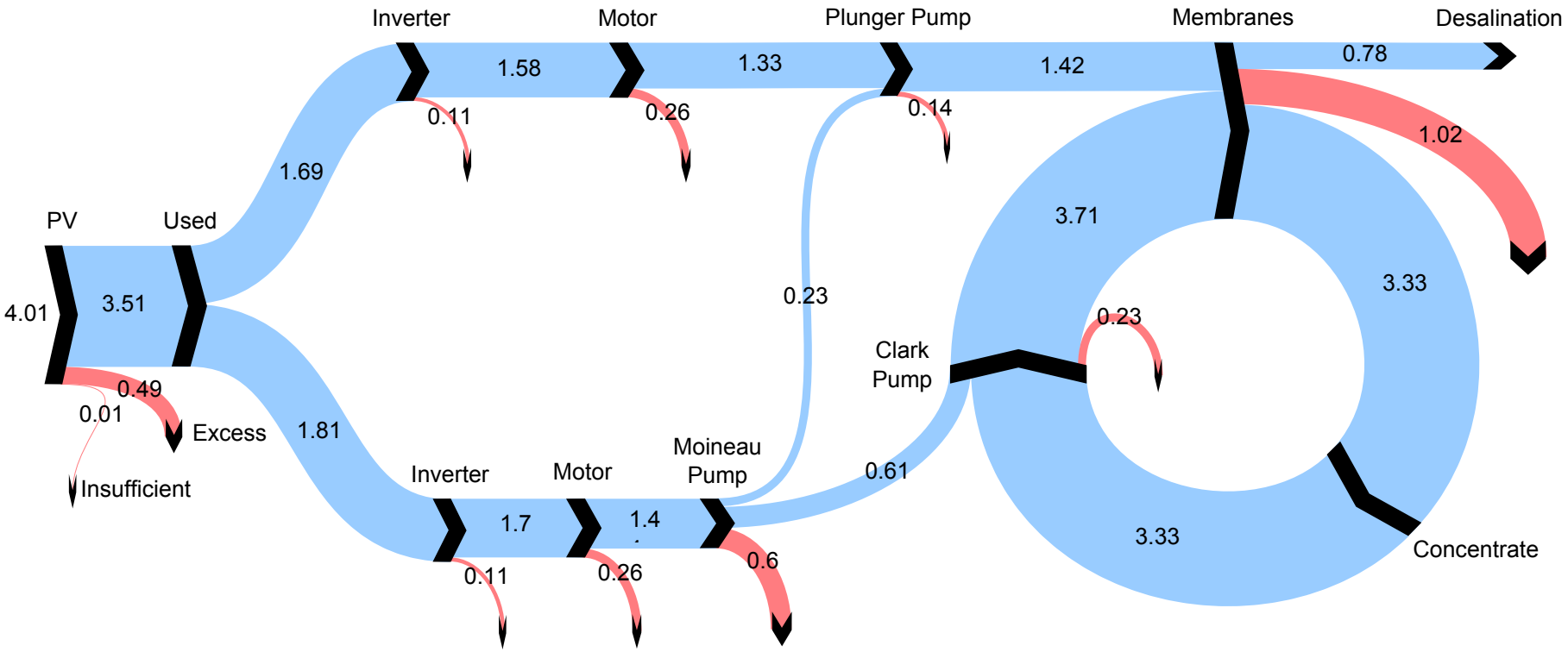

Figure 12 – Sankey Diagram – CREST Seawater PV-RO

Line widths and numeric values represent annual average specific energies in kWh/m^3.

Discussion

The Sankey diagram of Figure 12 represents the modelled energy flows through the hardware components shown earlier in Figure 11.

Starting at the left of Figure 12, we see two identified losses emanating from the **PV**. These losses occur, first, when there is **insufficient** power to run the RO rig, and second, when there is an **excess** of power available. In the absence of batteries, this energy is simply lost.

The energy that is used then divides roughly equally between the two inverter-motor-pump assemblies.

The **inverters** are industrial variable-frequency drives (VFD), which have no transformers or harmonic filtering, and are thus very efficient.

The **motors** are the highest-efficiency three-phase induction motors available from the major manufacturers. Even so, their losses are considerable due to their small size: 1.5 kW each.

The **Moineau pump** efficiency is approximately 57 % on average, over the variable flow and pressure operation in the PV-RO system. This efficiency is considerably higher than might be expected of a centrifugal pump operating with this duty.

The energy shown going from the Moineau pump to the plunger pump is by virtue of the pressure that the Moineau pump provides to the inlet of the plunger pump. The **plunger pump** itself is very efficient.

The **membrane** losses are quite high, compared for example to those shown for DESSOL. This is because, on average, the CREST system operates at a much lower water recovery ratio. This is also apparent in the relatively high proportion of energy in the concentrate stream.

The **Clark pump** recovers almost all the energy available in concentrate and returns it directly to the membrane feed. It achieves an average efficiency of over 94 %, which is excellent and allows the system to be operated at a relatively low water recovery ratio without sacrificing overall energy efficiency.

7 CREST Seawater Wind-RO, UK

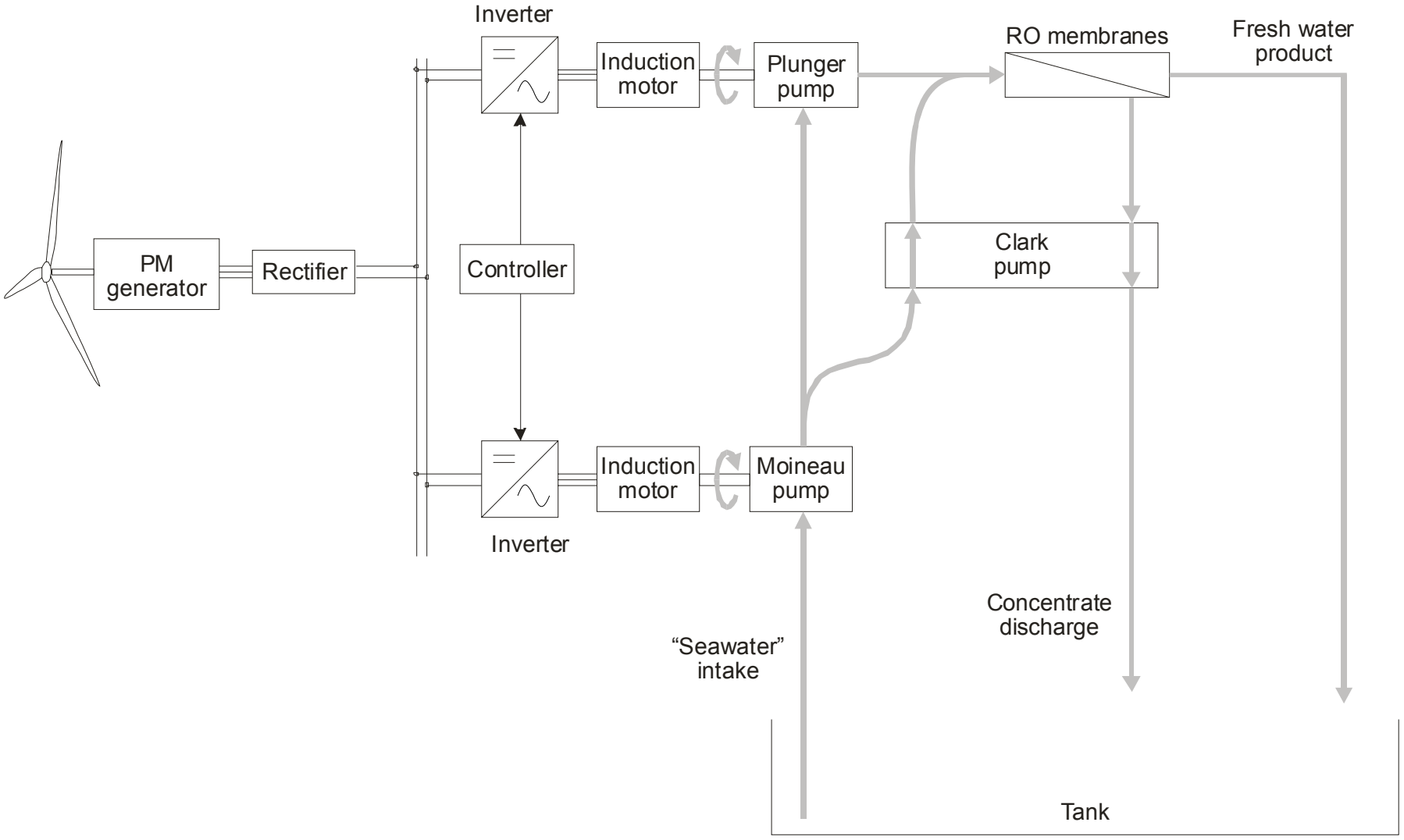

Figure 13 – General Arrangement – CREST Seawater Wind-RO

7.1 System details

The CREST seawater RO system has also been demonstrated operating directly from wind power without batteries[17]. The demonstration was brief, but did show that the rotational speed of the wind turbine could be controlled through the control of the inverters in the RO system. Wind turbulence caused much more rapid flow and pressure variations in the RO system than were seen with PV power. The modelling presented here does not attempt to represent these rapid variations. Instead, it uses hourly averaged data and assumes that this is adequate for calculation of average water production.

Wind speed data

Hourly data	Measured at RAL, Oxfordshire, UK.
Annual average	5.3 m/s

Assume hub height equals measurement height

Wind turbine

Manufacturer	Proven Energy	www.provenenergy.co.uk
Model	WT2500	http://www.provenenergy.co.uk/images/stories/PDFs/specifications.pdf
Rated power	2.5 kW	
Rotor diameter	3.5 m	
Gear box	None	
Generator	8-pole 3-phase permanent magnet	
Rotational speed	Variable up to 40 rad/s = 382 rpm	
Frequency	Variable up to 26 HzAC voltage (line-neutral)	Variable up to 220 V
DC voltage	Variable up to 575 V (limited before connection to inverters)	
Power curve	From manufacturer's datasheet, see also Miranda, page 64, Figure 2.17	

All other details: as per CREST PV-RO system

[17] Miranda, Marcos S. (2003). *Small-Scale Wind-Powered Seawater Desalination Without Batteries*, PhD, Loughborough University, UK. http://staff.bath.ac.uk/eesmm/Thesis.html

7.2 Modelled performance

General results from the model

Annual energy available from wind turbine	5247 kWh/y
Annual hours run	5950 h/y
Average hours run per day	16 h/d
Annual water production	1271 m^3/y
Average daily water production	3.48 m^3/d
Overall annual average specific energy	5247/1271 = 4.13 kWh/m^3

Given the annual average wind speed of 5.3 m/s, the annual energy available from the 2.5 kW Proven wind turbine is very similar to that available from the 2.4 kW_{peak} PV array in Eritrea. Thus, the annual yield and overall specific energy are also very similar. The hours run is increased, however, because the system spends more time operating at lower powers.

Sankey diagram

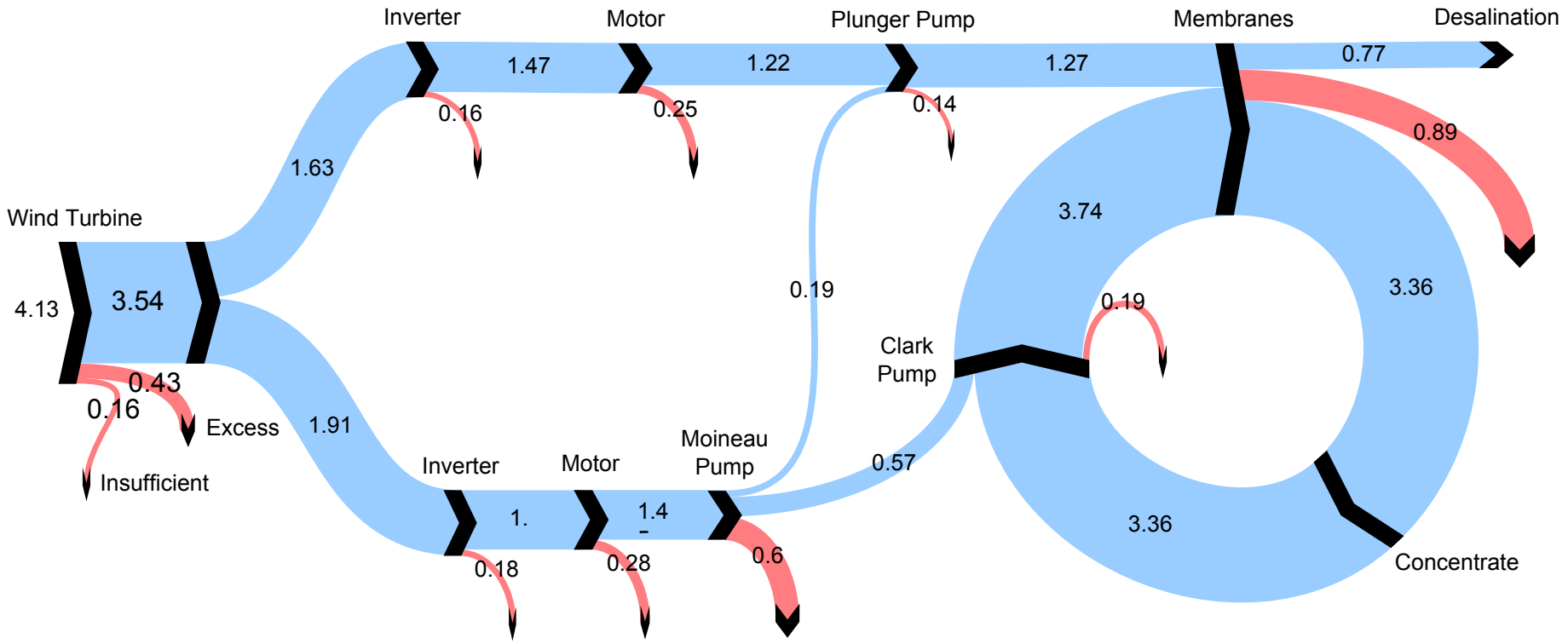

Figure 14 – Sankey Diagram – CREST Seawater Wind-RO
Line widths and numeric values represent annual average specific energies in kWh/m^3.

The Sankey diagram of Figure 14 is almost identical to the PV-powered system shown in Figure 12. The only significant differences are in the **insufficient** and **excess** powers.

8 ITN Brackish PV-RO, Mesquite, Nevada

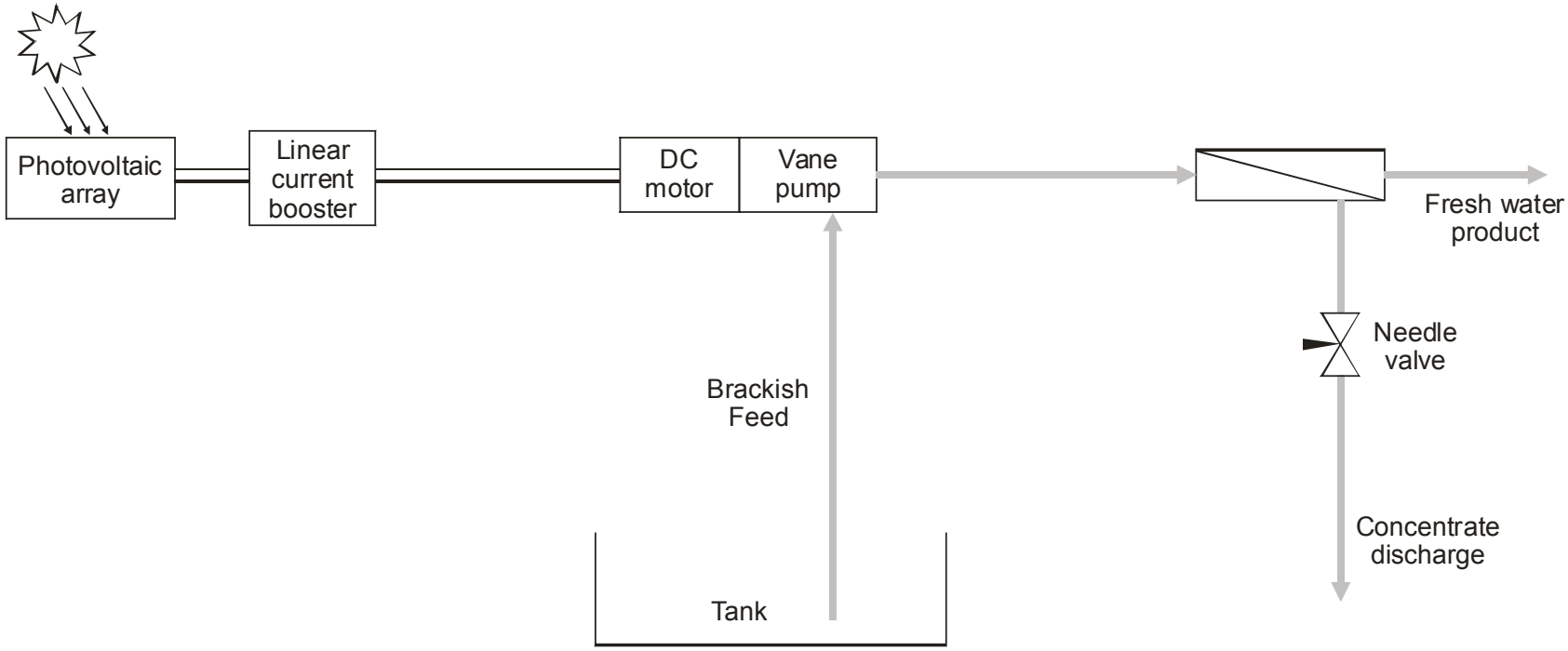

Figure 15 – General Arrangement – ITN Brackish PV-RO

8.1 Assumed details

The details given here were used for the modelling described in this report and may differ from those of the actual installed system.

The model is based on the brackish water PV-RO system described by Sing-Foong Cheah[18], operated in Mesquite, Nevada during 2003.

RO operational parameters

Product flow	Variable, up to 200 L/h
Recovery Ratio	Variable, up to 35 %
Working pressure	Variable, up to 14 bar

Feed water

Concentration	3622 ppm TDS (high Ca^{++} content)
…Osmotic pressure	1.52 bar
Iso-osmotic with	1900 mg/L NaCl solution
Feed temperature	21 °C to 33 °C (Figure 8 in the report). Modelled at 25 °C

Solar radiation

Hourly data	Meteonorm for Las Vegas	http://www.meteotest.ch/
Inclination	Equal to latitude	
Annual average	6.54 kWh/m^2/d	
Compares well with:		
Annual average tilted	6.5 kWh/m^2/d	http://rredc.nrel.gov/solar/old_data/nsrdb/redbook/sum2/23169.txt

[18] Cheah, Sing-Foong (2004). *Photovoltaic Reverse Osmosis Desalination System*, May 2004, ITN Energy Systems, Inc. www.usbr.gov/pmts/water/media/pdfs/report104.pdf

Photovoltaic array

Nominal array power	540 W_{peak}	
Nominal module power	60 W_{peak}	
Number of modules	9	
Wiring configuration	3 strings of 3 modules in series each	
Assume I-V curve details from:		
Manufacturer	Shell	
Model	SM50-H	http://www.scsolar.com/PDF_Files/ShellSM50-H_US.pdf
	But scaled to give 60 W_{peak} with 36 cells in series	

Motor and vane pump

Manufacturer	Dankoff Conergy	www.conergy.us
Range	Solar Slowpump	http://www.windsun.com/PDF/Solar_Slowpump_spec_Feb02.pdf
Model	1403 (22225)	
Rated battery voltage	48 V	

Linear current booster

Manufacturer	Dankoff Conergy	www.conergy.us
Model	DL-10A	http://www.windsun.com/PDF/Dankoff_LCB_specs.pdf
Current (max. continuous)	10 A	
Input voltage (nominal)	48 V	
Output voltage (up to)	60 V	
Efficiency at rated load	> 94 %	

RO membranes

Type	Spiral-wound, for brackish water	
Element size	2.5 inch by 40 inch	
Manufacturer	Osmonics (Now GE Osmonics)	www.osmonics.com
Model	Duraslick RO 2540	http://www.osmonics.com/...Specs-%20Duraslick%20RO%202540.pdf
Array configuration	4 membranes in series	
Assume energy performance similar to:		
Manufacturer	Dow FilmTec	http://www.dow.com/liquidseps/
Model	TW30-2540	http://www.dow.com/liquidseps/prod/tw30_2540.htm
Performance details	ROSA	http://www.dow.com/liquidseps/design/rosa.htm

A factor of 0.85 was used to match the ROSA data to that of the Duraslick.

8.2 Modelled performance

General results from the model

Annual energy available from PV	1075 kWh/y
Annual hours run	3604 h/y
Average hours run per day	9.87 h/d
Annual water production	545 m^3/y
Average daily water production	1.49 m^3/d
Overall annual average specific energy	1075/ 545 = 1.97 kWh/m^3

The ITN brackish PV-RO system achieves an average of nearly 10 hours of operation per day. This is because it is variable-flow and because the linear current booster provides maximum-power-point tracking. The average specific energy is lower than the other systems considered in this report because the feed water is brackish.

Sankey diagram

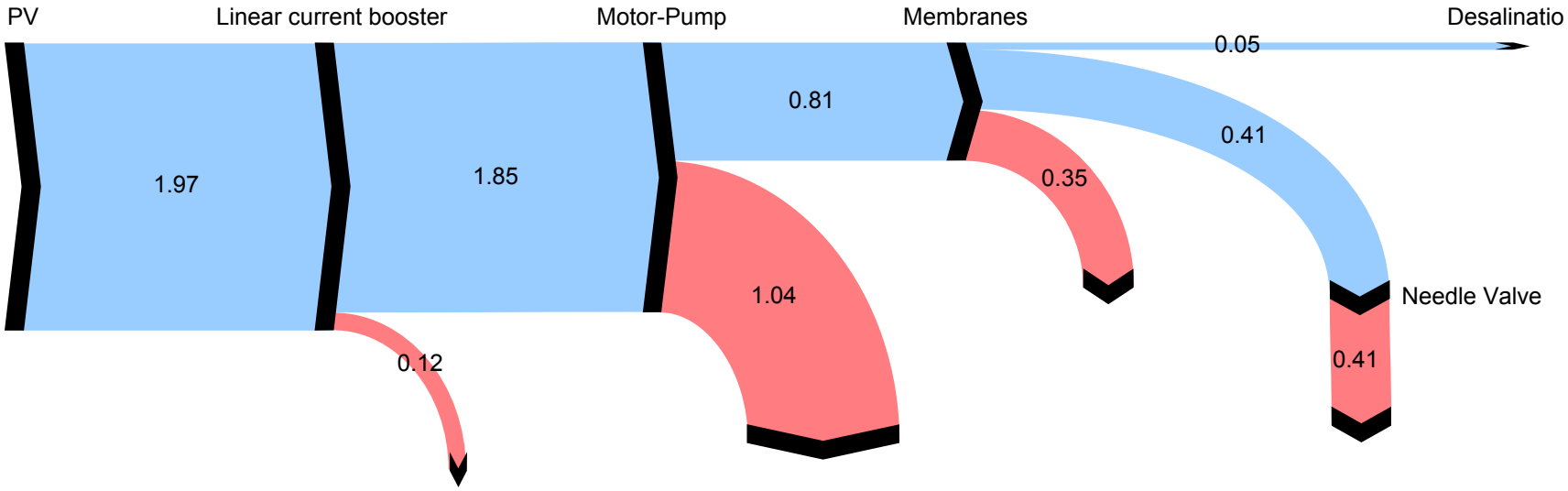

Figure 16 – Sankey Diagram – ITN Brackish water PV-RO, Mesquite, Nevada, USA.
Line widths and numeric values represent annual average specific energies in kWh/m^3.

Discussion

The Sankey diagram of Figure 16 represents the modelled energy flows through the hardware components shown earlier in Figure 15.

The energy generally moves from left to right along the blue paths. The losses from the individual components are indicated in red.

The **linear current booster** provides maximum-power-point tracking (**MPPT**), and thus extracts all of the power available from the **PV**. The power electronic DC-DC converter within the linear current booster does incur an energy loss, and the value shown is based on the manufactures efficiency data: ~ 94 %. Maximum-power-point tracking is particularly important in a system without batteries.

The motor-pump assembly comprises a **DC motor** driving a **vane pump**. It is modelled as a combined unit and represented as such in the Sankey diagram. Its electrical consumption is less than 400 W and its overall efficiency of around 44 % is actually quite good for such a small device.

The specific energy supplied to the **membranes** is much less than was seen earlier in the seawater systems. The membrane losses are also reduced but do represent a greater proportion of the whole.

As expected in a brackish water system, the energy in the **concentrate** which is dissipated in the **needle valve** is a smaller proportion of the whole, and the value of brine-stream energy recovery is less apparent. However, brine-stream energy recovery should not be dismissed because it allows operation at lower water recovery ratios, and thus reduces scaling potential. Scaling was found to be a problem in the ITN demonstration system at Mesquite.

9 INETI Brackish PV-RO, Portugal

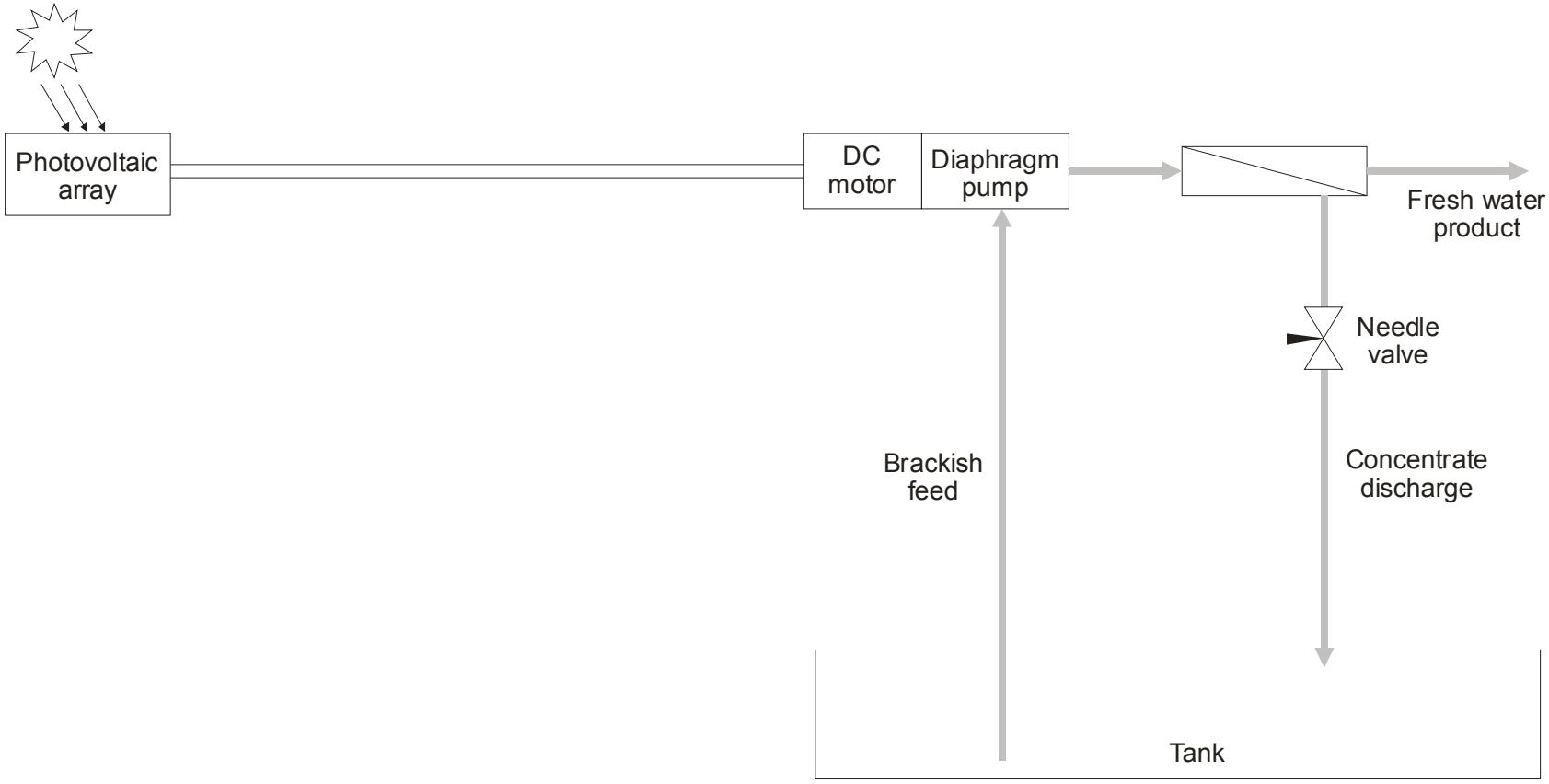

Figure 17 – General Arrangement – INETI Brackish PV-RO

9.1 Assumed details

The details given here were used for the modelling described in this report and may differ from those of the actual installed system.

The model is based on the system operated by INETI, Lisbon, Portugal [19, 20].

RO operational parameters

Product flow	Variable, up to 4.6 L/h
Feed flow	Variable, up to 190 L/h
… recovery ratio	less than 3 %
Working pressure	Variable, up to 4.2 bar

Feed water

Concentration	2000 mg/L NaCl solution
…Osmotic pressure	~ 1.8 bar
Feed Temperature	25 °C

Solar radiation

Hourly data	Meteonorm	http://www.meteotest.ch/
Inclination	Equal to latitude	
Annual average	5.22 kWh/m^2/d	
Compares well with:		
Annual average at 40°	5.44 kWh/m^2/d	http://re.jrc.cec.eu.int/pvgis/solradframe.php?lang=en&map=africa

[19] Joyce, Antonio, David Loureiro, Carlos Rodrigues and Susana Castro (2001). Small reverse osmosis units using PV systems for water purification in rural places. *Desalination* **137**(1-3): 39-44

[20] ADU-RES, Work package 2, Final report, section 4.3.1

Photovoltaic array

Nominal array power	150 W_{peak}
Number of modules	3
Nominal module power	50 W_{peak}
Module type	Mono-crystalline
Wiring configuration	3 modules in parallel

Assume details from:

Manufacturer	Atersa	
Model	A-50M	http://www.inrena.gob.pe/ianp/mantenimiento/manual_de_adquisiciones.pdf
Cells per module	36 in series	
Nominal module voltage	12 V	
MPP voltage	16 V	

I-V curve details scaled from:

Manufacturer	Atersa	
Model	A-75M	http://www.atersa.com/principalAtersaES.html

DC motor and diaphragm pump

Manufacturer	Shurflo	http://www.shurflo.com/.../8000-543-238.html
Voltage	12 V DC	

Assume details from:

Model	8000-543-238	http://www.depcopump.com/datasheets/shurflo/8000-543-238.pdf
Rated current	8.7 A	
… rated input power	104 W	

RO membrane

Number of elements	1	
Model	MP – TA50 – J4	
Material	Cellulosic compound	
Membrane type	Spiral wound	
Performance details scaled from:		
Manufacturer	Dow FilmTec	http://www.dow.com/liquidseps/
Model	TW30-2540	http://www.dow.com/PublishedLiterature/dh_058e/09002f138058e9d7.pdf...
Type	Spiral-wound, polyamide thin-film composite, for seawater	
Element size	2.5 inch by 40 inch	
Performance details	ROSA	http://www.dow.com/liquidseps/design/rosa.htm

9.2 Modelled performance

General results from the model

Annual energy available from PV	178 kWh/y
Annual hours run	2574 h/y
Average hours run per day	7.1 h/d
Annual water production	9.912 m^3/y
Average daily water production	0.027 m^3/d
Overall annual average specific energy	178/ 9.912= 17.96 kWh/m^3

Sankey diagram

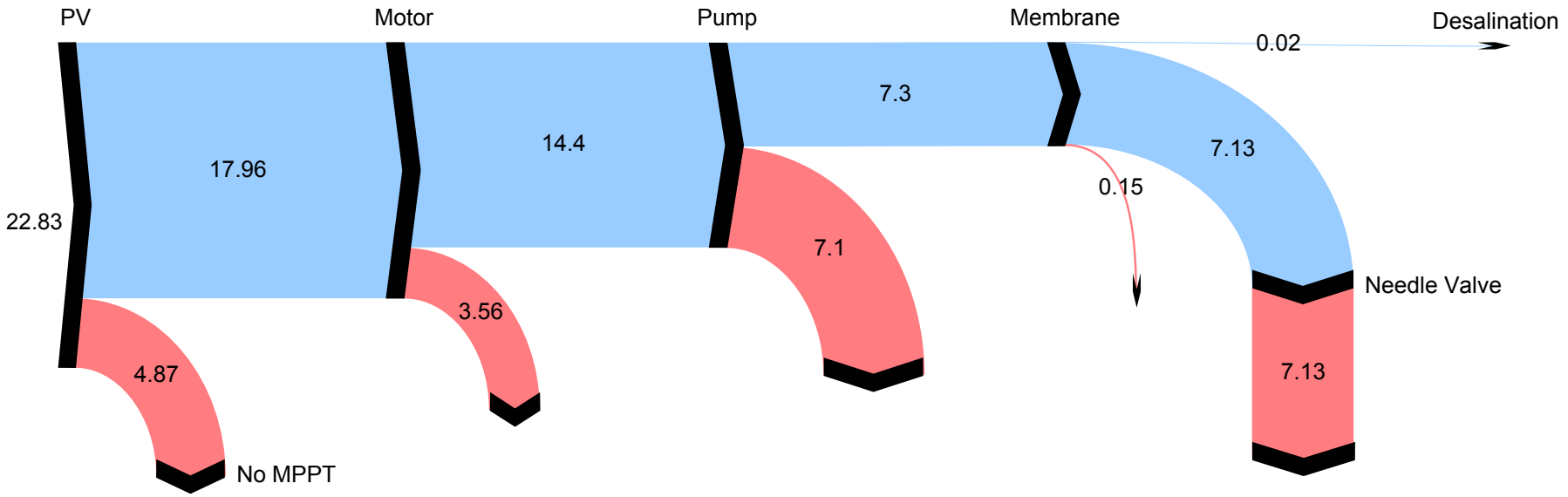

Figure 18 – Sankey Diagram – INETI Brackish PV-RO.
Line widths and numeric values represent annual average specific energies in kWh/m^3.

Discussion

The Sankey diagram of Figure 18 represents the modelled energy flows through the hardware components shown earlier in Figure 17.

The energy generally moves from left to right along the blue paths. The losses from the individual components are indicated in red.

The INETI system has a DC motor connected directly to the **PV**. There is no linear current booster and thus no maximum power point tracking (**MPPT**). Nor is there any battery, and thus the operating point on the PV's I-V characteristic is determined by the

motor's I-V characteristic. This, in turn, depends on the pump's torque-speed characteristic, and ultimately on the setting of the needle valve. Thus, the PV operating point is generally significantly away from the maximum power point, and the "no MPPT" losses are considerable. A linear current booster, as used in the ITN system, would virtually eliminate these losses and thus provide significantly more power to the motor. On the other hand, the same money could be spent on increasing the PV array size, which would have a similar effect. The respective cost-benefits have not been quantified here.

The Surflo motor-pump assembly comprises a **DC motor** driving a **diaphragm pump**. Its overall efficiency is around 41 % which is actually very good for such a small device: its electrical consumption ranges between about 20 W and 130 W.

As was the case in the ITN system, the **membrane losses** are roughly 7 times greater than the desalination energy. This is to be expected in brackish water systems.

Almost all (~ 97 %) of the energy presented to the membranes ends up in the concentrate and is lost in the **needle valve**. This is because the water **recovery ratio** is so low (below 3 %), as indicated in the published paper [21]. In most RO systems, the recovery ratio can be increased simply by closing the needle valve a little. This is true in the INETI system, but also alters the operating point on the PV's I-V characteristic and causes an increase in MPPT losses. For example, the model showed that closing the needle valve a little could increase the recovery ratio roughly threefold, whilst roughly doubling the MPPT losses; annual water production was increased only by 40 %. Alternatively, the system performance could be dramatically improved by the addition of membrane elements in series.

The sheer simplicity of the INETI system, as indicated in Figure 17, makes it very attractive: it has no batteries and no power electronics. However, it also creates a significant challenge in matching the component sizes to work efficiently over a wide range of solar irradiance.

[21] Joyce, Antonio, David Loureiro, Carlos Rodrigues and Susana Castro (2001). Small reverse osmosis units using PV systems for water purification in rural places. *Desalination* **137**(1-3): 39-44

10 Conclusions and recommendations

The Sankey diagrams presented in this report illustrate that the relatively high specific energy consumptions associated with small-scale RO systems are the result of losses in components throughout the systems. Lack of brine-stream energy recovery is the most significant factor but other losses can also be considerable.

The energy efficiency of PV and of RO membranes is almost independent of system size, and this gives the impression that small PV-RO systems will be efficient. Unfortunately, the energy efficiency of small motors and pumps can be very poor indeed, especially in the case of centrifugal pumps operated away from their best-efficiency point.

System design recommendations:

- Design and build larger systems, so as to avoid the very low efficiencies associated with small motors and pumps.
- Use energy recovery. The importance of using energy recovery is known to all RO system designers. The challenge with ADU-RES systems is that they tend to be rather small and the range of available energy-recovery devices is very limited. The best-known devices currently available are the Clark pump and its derivatives and the axial-piston motor.
- Minimize the energy going through the batteries and particularly avoid high charge and discharge rates.
- Use maximum-power-point tracking (MPPT) or ensure that the battery voltage is close to the MPP voltage at real operating temperatures.
- Check pump efficiencies over the intended operating range.
- For positive displacement pumps, ensure that both volumetric and mechanical efficiencies are accounted for.
- Consider using Moineau (progressing cavity) or vane pumps instead of centrifugal pumps. Moineau and vane pumps are positive displacement and generally give better efficiency, particularly if the pressure is variable. Note, however that they require a much higher starting torque.

- Use high-efficiency induction motors. The best-efficiency motors available from the major manufactures (ABB, Siemens, etc.) are significantly better than the standard motors usually supplied by pump manufacturers.
- Consider using slightly over-size motors: efficiencies are sometimes better at three-quarters load than at full load.

A more general recommendation is that the research and development of small-scale energy recovery devices be given a high priority.

This report has focused almost entirely on energy consumption. The assumption is that there is a strong relationship between specific energy consumption in kWh/m^3 and the final cost of water. Certainly, this is the case in systems where PV arrays costs are dominant. However, there does come a point where energy efficiency measures will actually cost more than the savings they can bring in PV array costs. Thus, it becomes necessary to shift the focus of the analysis towards a cost basis. A significant challenge in doing this is in the estimation of replacement times for items such as membranes and batteries.